


Article

The Evolution of Mosasaurid Foraging Behavior Through the Lens of Stable Carbon Isotopes

Michael J. Polcyn ^{1,2,*}, John A. Robbins ², Anne S. Schulp ^{1,3} , Johan Lindgren ⁴ and Louis L. Jacobs ² 

¹ Faculty of Geosciences, Utrecht University, Princetonlaan 8a, 3584CB Utrecht, The Netherlands; a.s.schulp@uu.nl

² Huffington Department of Earth Sciences, Southern Methodist University, Dallas, TX 75275, USA

³ Naturalis Biodiversity Center, Darwinweg 2, 2333CR Leiden, The Netherlands

⁴ Department of Geology, Lund University, Sölvegatan 12, 223 62 Lund, Sweden; johan.lindgren@geol.lu.se

* Correspondence: mpolcyn@smu.edu

Abstract: A large data set of new and previously published measurements of $\delta^{13}\text{C}$ values derived from tooth enamel ($n = 223$, of which 93 are new) are compiled to explore patterns of foraging area preferences of Late Cretaceous mosasaurid squamates over evolutionary time scales (~93–66 Ma). Our results indicate that small-bodied halisaurines are restricted to a relatively nearshore range, overlapping the lower end of the range of plioplatecarpines and some mosasaurine taxa. Most moderately sized plioplatecarpines occupy a relatively narrow foraging area in much of the nearshore and proximal offshore marine foraging area for the majority of their existence. Tylosaurines exhibit a greater offshore marine range than plioplatecarpines, consistent with their large body size and the robustness of their feeding apparatus. The largest tylosaurine taxa are replaced by *Mosasaurus* in the Late Campanian–Maastrichtian in the offshore foraging range. Mosasaurine taxa are found to occupy the broadest range of foraging areas, but their ranges are taxonomically segregated, consistent with adult body size and the diversity of feeding adaptations such as tooth morphologies and skull architecture seen in that subfamily. Where foraging areas of multiple taxa overlap, differences are typically in tooth form, reflecting prey preference or feeding niche. Foraging area occupation by multiple taxa with similar tooth forms suggests that other factors such as body size and prey acquisition style may have allowed for the finer partitioning of resources. Deep diving and long submergence may have also contributed to the depleted signals recovered for some of the large-bodied durophages and the largest of the macrophagous apex predators.

Keywords: paleoecology; foraging area; Mosasauridae; $\delta^{13}\text{C}$; stable carbon isotopes; Late Cretaceous



Academic Editors: Michael Wink and Nathalie Bardet

Received: 28 June 2024

Revised: 31 March 2025

Accepted: 15 April 2025

Published: 19 April 2025

Citation: Polcyn, M.J.; Robbins, J.A.; Schulp, A.S.; Lindgren, J.; Jacobs, L.L. The Evolution of Mosasaurid Foraging Behavior Through the Lens of Stable Carbon Isotopes. *Diversity* **2025**, *17*, 291. <https://doi.org/10.3390/d17040291>

Copyright: © 2025 by the authors. Licensee MDPI, Basel, Switzerland. This article is an open access article distributed under the terms and conditions of the Creative Commons Attribution (CC BY) license (<https://creativecommons.org/licenses/by/4.0/>).

1. Introduction

In this contribution, we report measurements of $\delta^{13}\text{C}$ derived from tooth enamel as a proxy for foraging area for a large temporal, geographic, and taxonomic sample of mosasaurs. Mosasaurs are an extinct clade of lizards that entered the marine realm at about 98 Ma and went extinct at the Cretaceous/Paleogene (K/Pg) boundary event at 66 Ma [1] (Figure 1). Early mosasaurs were morphologically similar to extant monitor lizards, and Mosasauria was recovered in recent phylogenetic analyses as the sister taxon to Varanoidea [2]. During their 32-million-year history, they adapted to life in water, undergoing significant morphological changes, most apparent in the development of flippers, fluked sculling tails, and a fusiform body shape [3]. Despite our increasing

knowledge of the morphology and phylogenetic relationships of mosasaurs, comparatively little is known of their feeding ecology. Most studies of this nature have used dental morphology and gut content to infer prey preference or the suitability of dentition to a particular prey type, but do not address the spatial segregation of their foraging area [4–20].

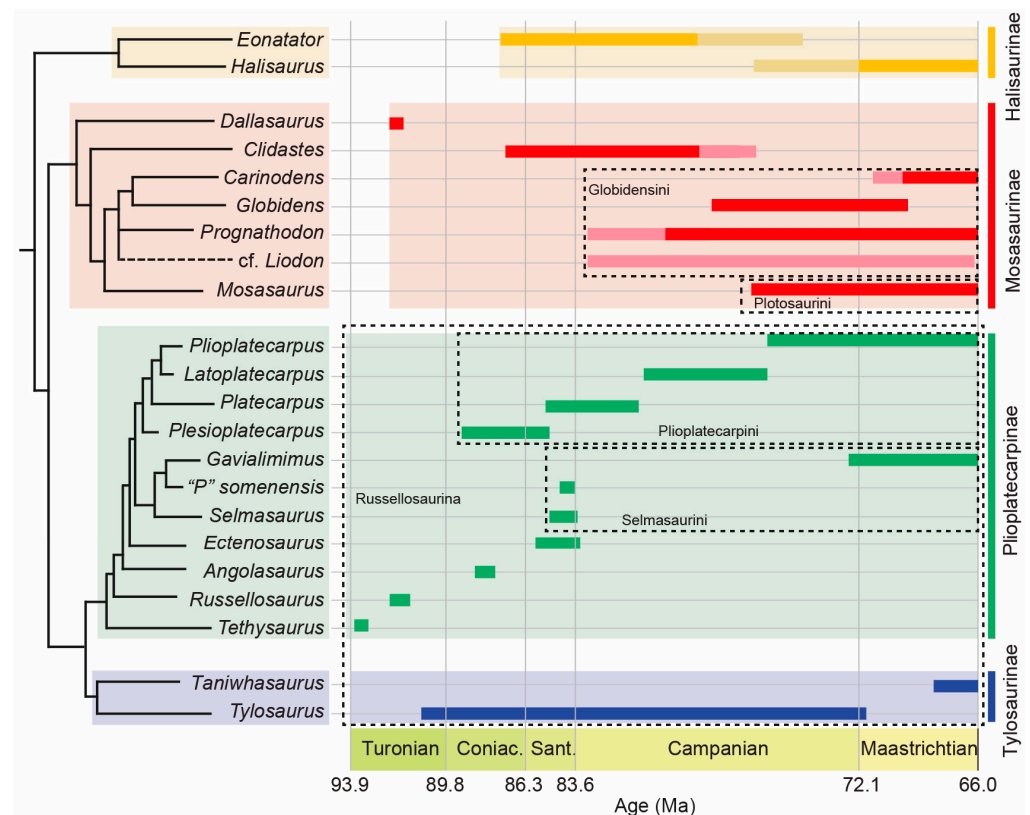


Figure 1. Simplified cladogram of mosasaurid relationships. See text for details.

Other studies have addressed the habitat preference of mosasaurs by inferring shore-line proximity and paleobathymetry from sedimentary analyses of the deposits in which mosasaur remains have been found [21–26]. Analyses of rare earth elements (REEs) have also been applied to mosasaur bones to infer the paleobathymetry of their habitats [27–29]. Although facies and REE analyses do provide clues as to the depositional environment in which the fossils are preserved, they do not necessarily reflect where the animals lived and foraged because of the possible postmortem transport of carcasses (e.g., [30]).

Conversely, carbon isotope measurements ($\delta^{13}\text{C}$) of marine vertebrates relate more directly to the diet [31] and foraging area [32] of the animal while alive. This is because marine primary producers have a wide range of $\delta^{13}\text{C}$ compositions reflecting the spatial gradient (nearshore to offshore) of particulate organic matter (POM; [33–35]). The ^{13}C -depleted nature of offshore primary producers propagates through the food web, causing larger, offshore-dwelling predators to have depleted $\delta^{13}\text{C}$ values compared to their nearshore counterparts. Clementz and Koch [32] used this phenomenon to identify differences in foraging zones between multiple marine, freshwater, and terrestrial mammals by analyzing the $\delta^{13}\text{C}$ values of tooth enamel.

Robbins et al. [36] were the first to explore mosasaur diet and foraging segregation through the examination of $\delta^{13}\text{C}$ values from tooth enamel, employing the methods of Clementz and Koch [32]. That study analyzed a small number of mosasaurine mosasaurs, a dolichosaurid, and the extant Galápagos marine iguana, *Amblyrhynchus cristatus*, and found that larger animals generally had lower $\delta^{13}\text{C}$ compositions, consistent with foraging farther from shore. Comparison with the isotopic ranges of tooth enamel $\delta^{13}\text{C}$ in mod-

ern pinnipeds grouped by foraging zone [32] revealed that smaller mosasaurs such as *Dallasaurus*, *Clidastes*, and juvenile *Globidens* had $\delta^{13}\text{C}$ values similar to modern kelp-bed-dwelling animals, with some specimens of *Clidastes* just bordering on the nearshore marine range. Larger mosasaurs, such as *Mosasaurus* and an adult *Globidens* from north Texas, fell within the nearshore marine range. Specimens of *Globidens* and *Prognathodon* from the Maastrichtian of Angola fell into the offshore range, which Robbins et al. [36] argued may have been the result of offshore foraging, deep diving (see below), or a combination of the two. Other studies [37–40] employed geographically and temporally restricted samples to infer resource partitioning in contemporaneous assemblages. In those studies, more-depleted $\delta^{13}\text{C}$ values were generally correlated with increased body size. Most recently, Leuzinger et al. [41] explored high-latitude stable isotopes, interpreting the composition of their mosasaur sample as an indication of a deeper, more offshore foraging area compared to the values recovered for their fish sample.

The simplified cladogram presented in Figure 1 is a synthesis of recent phylogenetic analyses [42–45]. Although there are a small number of basal branching, plesiopedal mosasaurids present in the Cenomanian and Turonian (~98 Ma–~90 Ma), most mosasaurids belong to one of four broadly recognized subfamilies (Halisaurinae, Tylosaurinae, Plioplatecarpinae, and Mosasaurinae) which appear to diverge in the Late Cenomanian or Early Turonian [43,46]. The compositions of the subfamily-ranked clades are relatively consistent among various workers, but the ingroup relationships of those subfamilies are somewhat more labile (e.g., [42–45,47–53]). Two additional subfamilies were erected by Palci and Caldwell [54] but not recovered in recent analyses [43,45], and the constituent taxa of those, along with *Ectenosaurus*, *Yaguarasaurus*, and *Angolasaurus*, are shown here as basal branching plioplatecarpines, but topologies may differ among analyses [42–44,51,55].

Later branching plioplatecarpines are included in the tribes Selmasaurini and Plioplatecarpini. Longrich et al. [45] erected the tribe Selmasaurini to include the genera *Selmasaurus*, *Gavialimimus*, *Goronyosaurus*, and *Khinjaria*, to which we provisionally add, here, “*Platecarpus*” *somenensis* Thevenin 1896. The tribe Plioplatecarpini was originally erected by Russell [21] to include the genera *Platecarpus*, *Plioplatecarpus*, and *Ectenosaurus*, but was revised by Longrich et al. [45] to include the genera *Plesioplatecarpus*, *Platecarpus*, *Latoplatecarpus*, and *Plioplatecarpus*, but not *Ectenosaurus*, as that taxon is more basal branching in their analysis (see also [52]). Species currently referred to *Ectenosaurus* are united by a number of characters unique among mosasaurids and likely form a monophyletic clade [55]; however, monophyly was not recovered in the strict consensus of recent analyses [55,56]. Our sample includes a single specimen (SMU76350) from Texas referred to the genus *Ectenosaurus* [57].

Mosasaurinae is a large and diverse clade that originates in the Turonian, represented by *Dallasaurus*, a small, plesiopedal taxon, recovered as a basal branching member of that clade [58]. The genus *Clidastes*, which we here consider monophyletic (but see also [59]), appears in the Coniacian and ranges into the middle Campanian [60]. In the Campanian, mosasaurines develop taxonomically disparate dental morphologies [1,61,62]. We use the tribe name Pliosaurini (sensu [47]) to include the genera *Mosasaurus*, *Plotosaurus*, *Jormungandr*, *Bentiabasaurus*, *Moanasaurus*, and *Rikisaurus*. Pliosaurini is the sister clade to the poorly resolved tribe Globidensini (sensu [47]), which includes the genera *Globidens*, *Prognathodon*, *Plesiotylosaurus*, *Thalassotitan*, certain taxa previously referred to the genus *Liodon* (fide [63]), and provisionally, *Carinodens*.

Halisaurinae has long been considered to have branched prior to the Mosasaurinae–Russellosaurina split [47,64]; however, some analyses recover Halisaurinae more closely related to Russellosaurina [50]. Halisaurines share a plesiomorphic configuration of the temporal arcade and quadrate suspensorium, a novel path for the internal carotid artery

in the parabasisphenoid, and complete paired nasals separating the premaxilla from the frontal, overlying the latter [65,66]. Given the plesiomorphic nature of this subfamily, we illustrate it in Figure 1 as branching basal to the Mosasaurinae–Russellosaurina split.

This study explores patterns of the foraging area preference of mosasaurs through time using $\delta^{13}\text{C}$ measurements from their tooth enamel. The data are compiled from both published and previously unpublished sources [36,37,39–41]. The sample includes species of four subfamilies, ranges in age from the lower middle Turonian (~92.5 Ma) to the Late Maastrichtian (~66 Ma), and includes specimens from North America (USA: Texas, Kansas, Arkansas), Israel, the Netherlands, Denmark, Sweden, Angola, Argentina, and Antarctica. We present the results by taxon and discuss patterns of foraging area segregation through time.

2. Materials and Methods

2.1. Sample Selection

A total of 93 new samples were analyzed for this contribution (see Appendix A for sample and replicate details). Teeth with good surface preservation and few cracks were preferentially selected to avoid breakage during the mechanical removal of the enamel, although incomplete teeth with broken bases or tips were also used, as these breaks made the identification of the dentine and enamel layers easier. One sample (*P. currii*) was recovered as enamel fragments left in a silicone mold of a single tooth of the holotype specimen. Where practical, molds of the teeth prepared for this study were made prior to sampling, and casts were deposited in the Shuler Museum of Paleontology at Southern Methodist University, Dallas, TX, USA. The mold of the *P. currii* tooth is housed at Lund University.

2.2. Sample Pretreatment

Teeth with adhesives on their exterior were first subjected to a 24 h suspension in acetone followed by vigorous rinsing and scrubbing with a soft brush before placement in a 0.1 M acetic acid solution for 72 h to remove diagenetic carbonate adhered to the surface of the tooth. This pretreatment method has been shown to remove diagenetic carbonate without affecting the original isotopic signature of the bioapatite [67]. The teeth were thoroughly washed again with deionized water, followed by two 20 min suspensions in an ultrasonic methanol bath to remove organic matter, and a third suspension in deionized water.

2.3. Sample Enamel Removal

After thorough drying, enamel was selectively removed using a low-speed rotary tool with a 0.5 mm tungsten carbide burr bit. The enamel was removed in passes and collected on sterile weigh paper and regularly transferred to a vial. The low-speed nature of the drill and regular collection of material assured that the specimen was not heated and that only enamel was collected. Any material that was present on the weigh paper when the drill struck dentin was discarded. One sample (*P. currii*) was only available as crushed material. Enamel was picked from this sample mechanically under a microscope to avoid the presence of any dentin.

2.4. Sample Analysis

For samples analyzed in the Stable Isotope Laboratory at Southern Methodist University, Dallas, TX, USA, between 0.7 and 5 mg of powdered enamel were reacted under vacuum with 102% phosphoric acid for at least 4 h at 25 °C before extraction on a vacuum line. Purified CO_2 gas was measured for isotopic composition on a Finnigan MAT 252 mass spectrometer and calibrated against a tank of carbon dioxide gas from Oztech Trading Corporation (Houston, TX, USA). This tank was periodically calibrated using a suite of

international (NBS-18 [$\delta^{13}\text{C}$ -5.01‰ , $\delta^{18}\text{O}$ -23.2‰], NBS-19 [$\delta^{13}\text{C}$ 1.95‰ , $\delta^{18}\text{O}$ -2.2‰]) and in-house (Carrara marble [$\delta^{13}\text{C}$ -2.2‰ , $\delta^{18}\text{O}$ -5.9‰]) carbonate standards.

Samples analyzed in the Stable Isotope Geosciences Facility at Texas A&M University, College Station, TX, USA, were weighed between 0.5 and 2 mg and reacted under vacuum with 102% phosphoric acid for ~15 min at 75 °C in a Kiel IV carbonate device coupled to a ThermoFinnigan MAT 253 mass spectrometer. These samples were run alongside multiple NBS-19 standards for calibration and quality control. Isotopic compositions are reported in δ -notation and expressed in part per thousand (‰) with respect to V-PDB. Analytical uncertainty from both labs was less than 0.1‰.

2.5. Compiled Data

The previously published data sets ($n = 130$ samples total) were run in different labs in the USA and Europe [36,37,39–41] using slightly different methods. For instance, samples were reacted at higher temperatures according to the methods of [37,40] than in the US labs [34,37, this study]. While there is concern about the high variability in oxygen isotopic compositions with different reaction temperatures and methods [68–70], the carbon isotopes, which are the focus of this study, show little variation when analyzed at different temperatures or through different techniques (see [70]) if the calibration methods are similar (i.e., one-point calibration; [71]). Each lab that measured the teeth reported their calibrated carbon isotopic compositions using international standards (SMU: NBS-18 [$\delta^{13}\text{C}$ -5.01‰ , $\delta^{18}\text{O}$ -23.2‰], NBS-19 [$\delta^{13}\text{C}$ 1.95‰ , $\delta^{18}\text{O}$ -2.2‰]; TAMU: NBS-19; UNIL: NBS-19; Vrije Universiteit (Amsterdam) Earth Science Stable Isotope Laboratory: IAEA-603 [$\delta^{13}\text{C}$ 2.46‰ , $\delta^{18}\text{O}$ -2.37‰]). This calibration step, along with the consistent behavior of carbon isotopic fractionation using different reaction temperatures and techniques, allowed us to compare results between labs. Isotopic compositions from each lab are reported in δ -notation and expressed in part per thousand (‰) with respect to V-PDB. Analytical uncertainty based on the standards run alongside the samples was 0.14‰ or better.

2.6. Taxonomic Identifications

The teeth in our new data set were identified to taxon by sampling from published specimens (e.g., [51,72]) or by comparison with specimens in institutional collections and descriptions and illustrations in the literature (e.g., [17,63,73–75]). The taxonomic identifications of samples from previous studies were maintained, with the exception of two samples referred to *Plioplatecarpus* [41], here considered *Taniwhasaurus* sp. based on comparisons with figured specimens [76]. We referred the teeth from Sweden to the taxon “*Platecarpus*” cf. “*P. somenensis*” because it compares well with the European holotype material of “*Platecarpus somenensis*” Thévenin 1896, which we consider a selmasaurin plioplatecarpine, and is not in reference to large North American plioplatecarpin plioplatecarpines that have been erroneously assigned to that taxon [47,52]. Species referred to the genus *Liodon* are considered to be closely related to or in some cases included in the genus *Prognathodon* [63]; however, we maintained the assignments to *Liodon* for the published samples [41] in our compiled data set.

2.7. Institutional Abbreviations

HUJ, Hebrew University of Jerusalem, Israel; LO, Paleontological Collection, Department of Geology, Lund University, Lund, Sweden; MGUAN PA, Museum of Geology, Universidade Agostinho Neto, Luanda, Angola; NHMM, Natuurhistorisch Museum Maastricht, Maastricht, the Netherlands; SMU, Shuler Museum of Paleontology, Southern Methodist University, Dallas, TX, USA.

3. Results

The detailed results are presented in Appendix A and graphically summarized in Figure 2. In the following sections, we present the findings by taxonomic group, placing them within foraging areas following the zonation scheme of Clementz and Koch [32]. We use the general terms “more nearshore” and “more offshore” to encompass the range of values from 0‰ to −16‰. We use the term “Nearshore Zone” (NSZ) to include the combined ranges of the “Kelp Bed Zone” (KBZ) and that portion of the “Estuarine Zone” (EZ) of Clementz and Koch [32] that falls below −8.0‰. We use “Nearshore Marine Zone” (NSMZ) and “Offshore Marine Zone” (OSMZ) for those partially overlapping zones defined by Clementz and Koch [32].

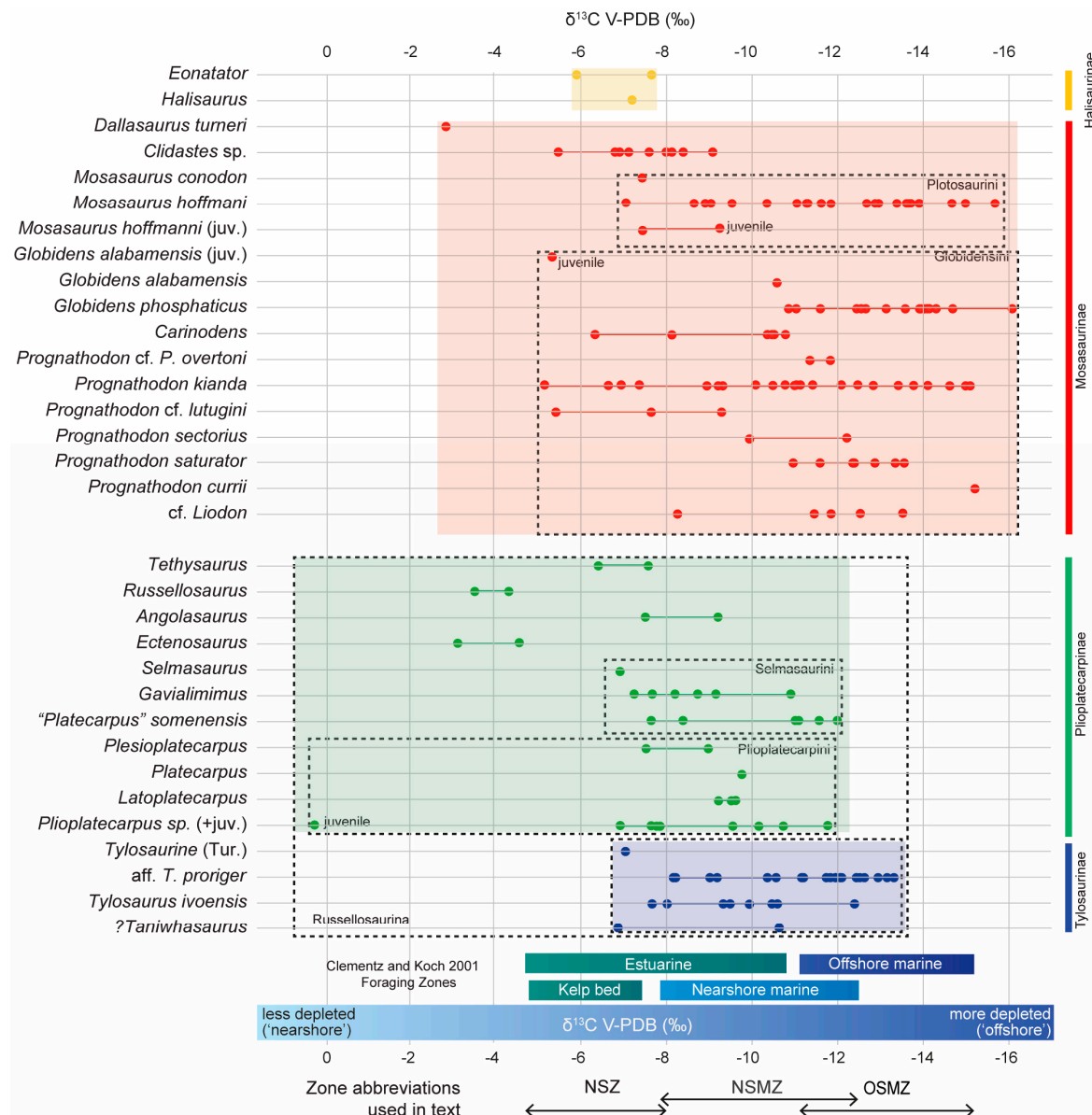


Figure 2. Mosasaurid $\delta^{13}\text{C}$ values by taxon. Color coding denotes subfamily membership: yellow = Halisaurinae; red = Mosasaurinae; green = Plioplatecarpinae; blue = Tylosaurinae. See Appendix A for details.

3.1. $\delta^{13}\text{C}$ by Taxon

3.1.1. Halisaurinae

Samples of *Eonatator* sp. from the latest early Campanian of Åsen, Sweden, yielded $\delta^{13}\text{C}$ values of -5.9 and -7.7‰ , and *Halisaurus* sp., from the Lower Maastrichtian of Angola [39], yielded a value of -7.2‰ , suggesting foraging in the NSZ.

3.1.2. Early-Diverging Plioplatecarpinae

Tethysaurus nopscai, from the lower Turonian of Morocco, with an average $\delta^{13}\text{C}$ value of -6.9‰ , suggests a NSZ preference. *Russellosaurus coheni*, from the middle Turonian of Texas ranged from -3.5‰ to -4.3‰ , suggesting foraging in the least depleted NSZ, exceeding the ranges given by [32]. *Ectenosaurus* sp. from the upper Santonian of west Texas [57] had a range of -3.1‰ to -4.6‰ , indicating foraging in the most enriched NSZ and similar to the results for *Russellosaurus*. *Angolasaurus bocagei* from the Coniacian of Angola [74] yielded values of -7.4‰ to -9.2‰ , within the range of later branching plioplatecarpines and within the NSMZ.

3.1.3. Plioplatecarpinae: Plioplatecarpini

Three North American plioplatecarpines yielded values between -7.5‰ and -9.6‰ , falling within the lower half of the NSMZ. *Plesioplatecarpus* sp. from Kansas and Texas yielded -8.8‰ and -7.5‰ , respectively. *Latoplatecarpus* sp. from Kansas yielded -7.6‰ and the Texas sample yielded a range of values from -9.1‰ to -9.6‰ . *Plioplatecarpus* sp. from north central Texas and western Arkansas yielded -7.6‰ and -7.7‰ , respectively. The northern European *Plioplatecarpus* samples yielded a range from about -7.0‰ to -11.1‰ . One Scandinavian *Plioplatecarpus* sample yielded -9.5‰ , while a juvenile sample yielded a value of -0.2‰ , which appears to be an outlier and is likely diagenetically altered. Apart from the aforementioned outlier, most *Plioplatecarpus* samples fall within the NSMZ, but the European–Scandinavian sample's upper range is more depleted than the North American sample.

3.1.4. Plioplatecarpinae: Selmasaurini

Three selmasaurin taxa yielded a range of values from -6.9‰ to -11.5‰ . *Selmasaurus johnsoni* from the lower Santonian of western Kansas yielded -6.9‰ , falling within the NSZ. Three specimens of the selmasaurin "*Platecarpus*" cf. "*P.*" cf. *somenensis* from the lower Campanian of Åsen, Sweden, had average $\delta^{13}\text{C}$ ratios of -10.9‰ , -11.3‰ , and -11.5‰ , within the overlapping part of the NSMZ and the OSMZ, the most depleted (offshore) values of any plioplatecarpine. An individual from Ugnsmunnarna, Sweden, also lower Campanian, had an average value of -7.7‰ , within the distal part of the NSZ. *Gavialimimus* sp. [20] from the Lower Maastrichtian of Bentiaba, Angola, yielded values ranging from -7.2‰ to -10.9‰ , suggesting that it was foraging in much of the NSMZ.

3.1.5. Tylosaurinae

An undescribed basal branching tylosaurine from the Turonian of North Texas (LO7786) yielded a $\delta^{13}\text{C}$ ratio of -7.0‰ , indicating foraging in the depleted portion of the NSMZ. Eight specimens of *Tylosaurus* aff. *T. proriger* yielded values ranging from -8.2‰ to -13.3‰ , occupying most of the NSMZ but extending into the more depleted portion of the OSMZ. Nine samples of *Tylosaurus ivoensis* from Åsen, Sweden, yielded average $\delta^{13}\text{C}$ ratios between -7.6 and -12.4‰ , suggesting foraging primarily in the NSMZ, but also ranging into the OSMZ.

3.1.6. Early-Diverging Mosasaurinae

The basal branching mosasaurine *Dallasaurus turneri* from the middle Turonian of Texas yielded a $\delta^{13}\text{C}$ value of -2.8‰ , suggesting foraging in the most enriched NSZ, similar to the results for *Russellosaurus* and *Ectenosaurus*. *Clidastes* from Texas yielded values ranging from -6.7‰ and -8.3‰ , and *Clidastes* from Åsen, Sweden, ranged from -5.4‰ to -9.1‰ , indicating that *Clidastes* was foraging in the NSZ and the less depleted portion of the NSMZ.

3.1.7. Mosasaurinae: Plotosaurini

A single specimen of *Mosasaurus conodon* yielded a value of -7.4‰ , foraging in the most depleted part of the NSZ. Adult specimens of *Mosasaurus hoffmanni* ranged from -7.1‰ to -14.9‰ , with specimens from Texas yielding values from -7.4‰ to -9.5‰ , the Netherlands -7.1‰ to -14.9‰ , and Angola from -8.9‰ to -12.9‰ , ranging through all three foraging zones and beyond the OSMZ. Juvenile specimens of *M. hoffmanni* from northern Europe yielded values of -7.1‰ to -9.2‰ , ranging from the most depleted part of the NSZ to the less depleted quarter of the NSMZ.

3.1.8. Mosasaurinae: Globidensini

A juvenile *Globidens alabamaensis* yielded an average $\delta^{13}\text{C}$ value of -5.3‰ , at the most enriched end of the NSZ. A co-occurring adult specimen of *G. alabamaensis* yielded an average value of -10.5‰ , in the lower part of the more depleted half of the NSMZ. Samples of *Globidens phosphaticus* teeth from the Lower Maastrichtian of Bentiaba, Angola, yielded average $\delta^{13}\text{C}$ values ranging from -10.8‰ and -16.1‰ , falling mostly within, but also exceeding, the OSMZ. *Carinodens* from the Upper Maastrichtian of northern Europe yielded values ranging from -10.3‰ to -10.8‰ ; a single sample from Denmark yielded -6.3‰ and a single Angolan sample yielded -8.1‰ . Taken together, these suggest that *Carinodens* foraged in the upper half of the NSZ and much of the NSMZ. A single specimen of *P. currii* from the latest Campanian of Israel gave a single measurement of -15.1‰ , falling within the most depleted portion of the OSMZ.

A *Prognathodon* cf. *P. overtoni* specimen from the Lower Maastrichtian of north Texas had a $\delta^{13}\text{C}$ average value of -11.5‰ [36], falling within the overlapping portions of the NSMZ and OSMZ. Two specimens of *Prognathodon* cf. *P. lutugini* from the middle Campanian of Åsen, Sweden, yielded $\delta^{13}\text{C}$ values between -5.4‰ and -9.3‰ , ranging from the NSZ into the lower half of the NSMZ. *Prognathodon sectorius* from the Maastrichtian of northern Europe yielded $\delta^{13}\text{C}$ values of -9.9‰ to -12.2‰ , approximately in the upper half of the NSMZ and the overlapping, less depleted part of the OSMZ. *Prognathodon saturator* from the Maastrichtian of northern Europe yielded values ranging from -10.9‰ to -13.6‰ , falling within the more depleted part of the NSMZ and ranging into the upper half of the OSMZ. *Prognathodon kianda* from the Lower Maastrichtian of Bentiaba, Angola, ranged from -5.2‰ to -15‰ , suggesting foraging across all three defined zones. Specimens tentatively referred to *Liodon* from Antarctica ranged between -8.2‰ and -13.5‰ , encompassing the NSMZ and ranging into the upper half of the OSMZ.

3.2. $\delta^{13}\text{C}$ Through Time

Figure 3 illustrates the geographic distribution of mosasaurs and feeding guild coverage [8,17,37,77] for five time slices and $\delta^{13}\text{C}$ values by taxon through time, ranging from the early middle Turonian (~93 Ma) though to the latest Maastrichtian (66 Ma), for the taxa analyzed in this contribution.

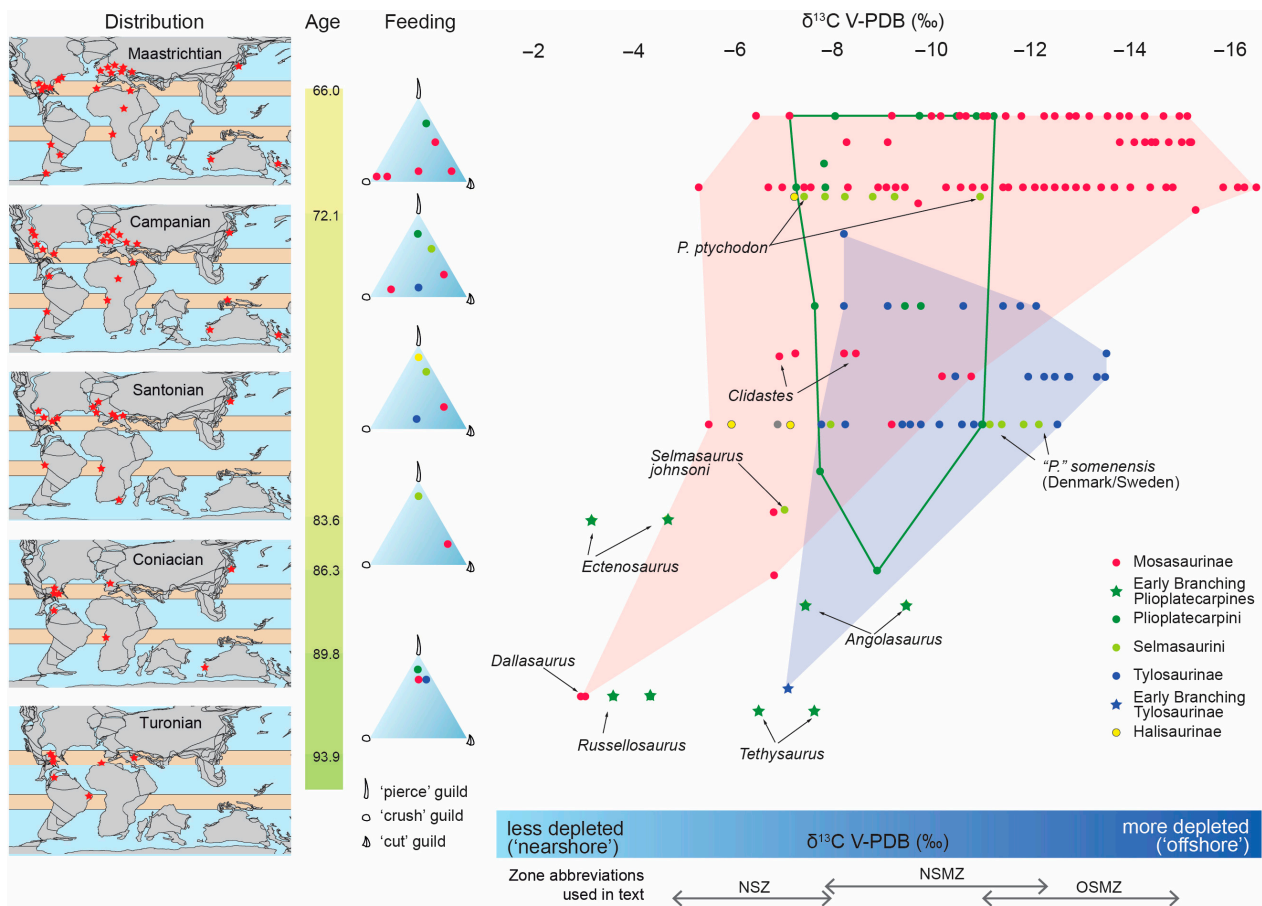


Figure 3. Temporal distribution of mosasaurs, tooth guild occupation, and isotope values by taxon. Geographic distribution of mosasaurs through time after [1]; horizontal tan bands span 15° to 30° north and south latitude. Tooth-morphology-based guild membership is subjectively assessed following previous research [8,17,77]. Color denotes subfamily membership: yellow = Halisaurinae; red = Mosasaurinae; green = Plioplatecarpinae; blue = Tylosaurinae.

3.2.1. Early Radiations

Foraging area segregation at the subfamily level appears to be established by the lower middle Turonian. Early-diverging plioplatecarpines, such as *Tethysaurus* and *Russellosaurus*, range farther offshore than *Dallasaurus*, which is also differentiated by its small size (~1 m) and tooth form [58]. *Tethysaurus* has the most depleted values, falling within the NSMZ (but see discussion below). A three-to-four-meter-long basal branching tylosaurine from the upper part of the middle Turonian of Texas occupies the proximal part of the NSMZ, but also maintains a conservative dentition, similar to *Russellosaurus* in size and shape.

3.2.2. Coniacian–Santonian

By the Coniacian–Santonian, most moderately sized plioplatecarpines, such as *Angolasaurus*, fall within the NSMZ, a foraging range they occupy through the remainder of the Cretaceous. Exceptions to this include the rare taxa *Ectenosaurus*, *Selmasaurus*, and “*P.*” cf. *somenensis*, all of which deviate from contemporaneous plioplatecarpines in dental morphology, skull architecture, or both. Within the Coniacian–Santonian sample, *Clidastes* is the first mosasaur bearing blade-like teeth. Although *Clidastes* is approximately the same adult size as contemporary plioplatecarpines, it appears to prefer a more nearshore foraging area. However, there are only a couple of contemporary plioplatecarpine samples and no tylosaurine samples for this interval, limiting direct comparisons.

3.2.3. Campanian

In the middle Campanian, most plioplatecarpin plioplatecarpines fall within the NSMZ, as in the prior and following stages. The exceptions to this are the early occurrences of *Plioplatecarpus* which appear in the upper Campanian of the North American Gulf Coast, with our samples from Texas and Arkansas falling within the most distal part of the NSZ. Also in the Campanian, tylosaurines achieve gigantic proportions [1] and range from the NSMZ into the proximal two-thirds of the OSMZ. *Clidastes* maintains a relatively nearshore habitat and is present into the middle Campanian, but is not known from the upper Campanian or thereafter. In the lower and middle Campanian, mosasaurines show a marked increase in taxonomic diversity and morphological disparity (Figure 1; [1]), with the first appearance of globidensin mosasaurines represented by *Prognathodon*, *Liodon*, and the durophagous *Globidens*. The first appearance of a plotosaurin mosasaurine is *Mosasaurus conodon*, with our sample falling within the foraging range of *Clidastes*. The body size and dentition of *Mosasaurus conodon* is similar to that of the large middle Campanian *Clidastes*, which it likely replaced in that feeding niche in the later part of the Campanian. *Prognathodon* cf. *P. overtoni* falls within the proximal part of the OSMZ and bears a robust crush-cut guild dentition, while *Prognathodon* cf. *P. lutugini* falls within the NS and NSMZ, has a sectorial dentition, and falls within the cut guild. *Globidens* is found in the NSZ and NSMZ and bears a nearly hemispherical crushing dentition in the middle tooth row.

3.2.4. Maastrichtian

In the Maastrichtian, plioplatecarpin plioplatecarpines are represented by *Plioplatecarpus* from northern Europe in our sample set. They fall within a slightly expanded range compared to previous stages, in the distal part of the NSZ and spanning the entire NSMZ. This is also the case for the selmasaurin *Gavialimimus* sp. from the Maastrichtian of Angola. The large plotosaurin mosasaurine *Mosasaurus hoffmanni* also appears in the Maastrichtian and occupies the distal NSZ to beyond the defined limit of the OSMZ. This taxon is similar to *Tylosaurus* in size and dental morphology, completely overlaps with its foraging range, and thus appears to be the ecological replacement for large tylosaurines, which are not known after the Early Maastrichtian.

A remarkable increase in disparity in tooth morphology occurs in Globidensini. There is increased taxonomic diversity in durophagous taxa with the appearance of large-bodied, low-crowned durophages such as *Globidens phosphaticus*, the high-crowned durophage *Prognathodon currii*, and small-bodied taxa such as *Carinodens*. There is also significantly expanded taxonomic diversity and tooth disparity in large macrophagous taxa such as *Prognathodon saturator* and a range of other forms bearing more or less sectorial dentitions but varying in their degree of lateral compression, such as in the taxa *Prognathodon sectorius* and *P. kianda*. The Maastrichtian durophagous taxa in our sample are both relatively depleted. *Globidens phosphaticus* ranges from the distal part of the NSMZ to beyond the OSMZ, the most depleted (offshore) values for any taxon in our sample. Our single sample of *P. currii* falls in the most depleted part of the OSMZ. *P. saturator* and *P. sectorius* (which overlap the more enriched part of the range of *P. saturator*) fall within approximately the middle of the foraging range recovered for the contemporaneous *M. hoffmanni*. However, those three co-occurring taxa differ from one another in tooth morphology [37,78] and, in the case of *P. saturator*, in skull architecture as well [79].

4. Discussion

4.1. Trophic Level and Foraging Habit

Based on tooth form and known gut content, the mosasaur taxa discussed here were carnivorous [8,17,20,77]. To facilitate comparisons between taxa, we assume dietary fractionation was the same for all taxa. Fractionation factors from diet to enamel ($\alpha_{\text{diet-enamel}}$) vary less among carnivores compared to herbivorous taxa (see [80,81]), typically centering around 9‰ for terrestrial carnivores [82,83] and ~10‰ for modern odontocetes [84–87]. While enrichment in whole-body ^{13}C occurs from one trophic level to the next, its relevance is relatively minor (up to 1‰ per trophic step, [31]). The opposite is true for $\delta^{13}\text{C}_{\text{POM}}$ values, which become more depleted (increasingly negative) with distance from shore and with depth, which propagates depletion from primary producers to top predator $\delta^{13}\text{C}$ enamel values through the trophic chain [32].

Foraging depth may also be a factor in interpreting $\delta^{13}\text{C}$ values. Benner et al. [88] demonstrated a decrease in primary producer $\delta^{13}\text{C}$ of about 3‰ between waters 100 to 200 m deep. This decrease in primary producer $\delta^{13}\text{C}$ with increasing depth propagates through the food web, resulting in carnivores that consistently feed at depth having depleted $\delta^{13}\text{C}$ ratios compared to shallow-foraging individuals. For example, Clementz and Koch [32] argued that the depleted nature of elephant seal tooth enamel $\delta^{13}\text{C}$ (~−13‰) relative to other pinnipeds may be in part related to their habit of deep diving (>300 m, with some dives exceeding 1000 m [89]). Thus, we interpret $\delta^{13}\text{C}$ values primarily as a proxy for foraging area, which may indicate shoreline proximity, water depth, or some combination of the two.

4.2. Physiological Factors

Air-breathing marine amniotes accumulate CO_2 in their bodies during oxygen consumption while breath-holding [90–92]. This increased amount of respired CO_2 in the blood among deep divers (or long-duration breath-holding) leads to a more depleted $\delta^{13}\text{C}$ value compared to shallow-diving or surface-dwelling individuals. During long-term dives, marine reptiles may increase the accumulation of CO_2 in their body fluids, including the blood, as a result of the increased resistance to blood flow [90,93,94]. The CO_2 present in the blood then reacts with water, forming carbonic acid. This acid dissociates into carbonate and bicarbonate (HCO_3^-), the latter being the predominant form of CO_2 in the blood [91]. The majority of bone and enamel carbonate is derived from the respired CO_2 in the blood. Thus, the ^{13}C -depleted nature of respired CO_2 results in a negative correlation between the amounts of respired CO_2 incorporated in bone carbonate and the $\delta^{13}\text{C}$ of that carbonate [95].

Physiological differences between shallow and deep divers may influence the fractionation captured in tooth enamel. Deep-diving marine amniotes typically store more oxygen in their blood and tissues than their lungs [94]. During long, deep dives, oxygen release is favored over oxygen uptake, which efficiently uses stored oxygen and increases the amount of respired CO_2 in the blood. The ^{13}C -depleted respired CO_2 is then incorporated into the tissue carbonate. Shallow divers lack the deep-diving adaptation of increased oxygen storage in the blood and tissues, instead storing more oxygen in the lungs [94]. During long dive periods, blood pH decreases. This pH decrease occurs in tandem with the decrease in pO_2 in the lungs, a situation which favors oxygen uptake rather than release. The Bohr effect, a decrease in oxygen affinity with decreasing pH, is disadvantageous under these long, shallow dive conditions. The Bohr effect decreases over the course of a prolonged dive to compensate for the drop in pH, which allows for the release of the last traces of O_2 in the lungs [94]. This method is a less efficient oxygen transport system than that of deep-divers, resulting in lower amounts of respired CO_2 in the blood compared to deep-diving species.

The carbonate precipitated in equilibrium with the blood of a shallow-diving animal should therefore be enriched in ^{13}C compared to deep-divers.

Biasatti [96] examined modern sea turtle remains for evidence of the effects of respiratory physiology, diet, and latitude on the $\delta^{13}\text{C}$ ratios of sea turtle bone carbonate. Samples from the Green sea turtle, *Chelonia mydas*, a shallow-diving species, were similar to those of barnacles found on their carapaces and the $\delta^{13}\text{C}$ ratios of marine dissolved inorganic carbonate (DIC; 0–1‰). Biasatti [96] also argued that the deep-diving adaptations and behavior of Leatherback (*Dermochelys coriacea*) and Olive Ridley (*Lepidochelys olivacea*) sea turtles cause a greater accumulation of CO_2 in the blood compared to species not adapted for deep diving. The depleted values from the Leatherback turtle (−6 to −13‰) and Olive Ridley turtle (−7 to −9‰) were similar to the ranges found among deep-diving cetaceans [96,97].

Although carbon isotope ratios may be influenced by depth [88] and dive duration [95,96], when viewed in the context of depositional environment or other clues as to feeding style, these factors may provide more nuanced interpretations of the raw $\delta^{13}\text{C}$ values in certain taxa. One example is the large Maastrichtian durophage *Globidens phosphaticus* and the locality of Bentiaba, Angola [73]. Skeletal remains and numerous shed teeth are found within a small geographic area at Bentiaba, associated with the remains of other taxa which yielded much more enriched $\delta^{13}\text{C}$ values [39]. Thus, shoreline proximity alone cannot account for the depleted values seen in *Globidens phosphaticus* (−11 to −16‰). The depositional setting in the locality is relatively nearshore and the local paleobathymetry is estimated to be 50–150 m [39]. The taxon possesses large, irregularly hemispherical teeth, well suited for crushing hard-shelled prey. The locality is also rich in the remains of a large inoceramid bivalve, reported to be at least one of the prey items of the genus [12]. Taken together, it is reasonable to infer that at least part of the significantly depleted values seen in this taxon is due to the increased dive time (and depth) associated with bottom foraging. Additionally, feeding low on the trophic chain, *Globidens* would not manifest the 1‰ per trophic step enrichment of the apex predators in the ecosystem, given comparable shoreline proximity.

4.3. Other Factors

Local ecological setting and latitude are known to affect $\delta^{13}\text{C}$ values. However, patterns of mosasaur assemblages in disparate geographies (and time slices) of our data are broadly similar (Figure 4), with larger taxa generally exhibiting more depleted values (Figure 5). This body-size partitioning correlates well with tooth forms, where small-bodied piscivorous taxa occupy a more nearshore range, large-bodied macrophages forage in a more offshore range, and generalists with more or less sectorial dentitions foraging in a broad range irrespective of body size (e.g., *Prognathodon kianda*). Where two taxa are found to occupy the same isotopic range, there is little or no overlap in tooth form. Where differences between similar taxa occur between localities, these may be an artifact of noise in the sample, local ecological effects related to shoreline proximity, latitude, or some combination of these. Nonetheless, the broader patterns of foraging area partitioning are relatively consistent, although comparisons among geographies reveal some differences in detail.

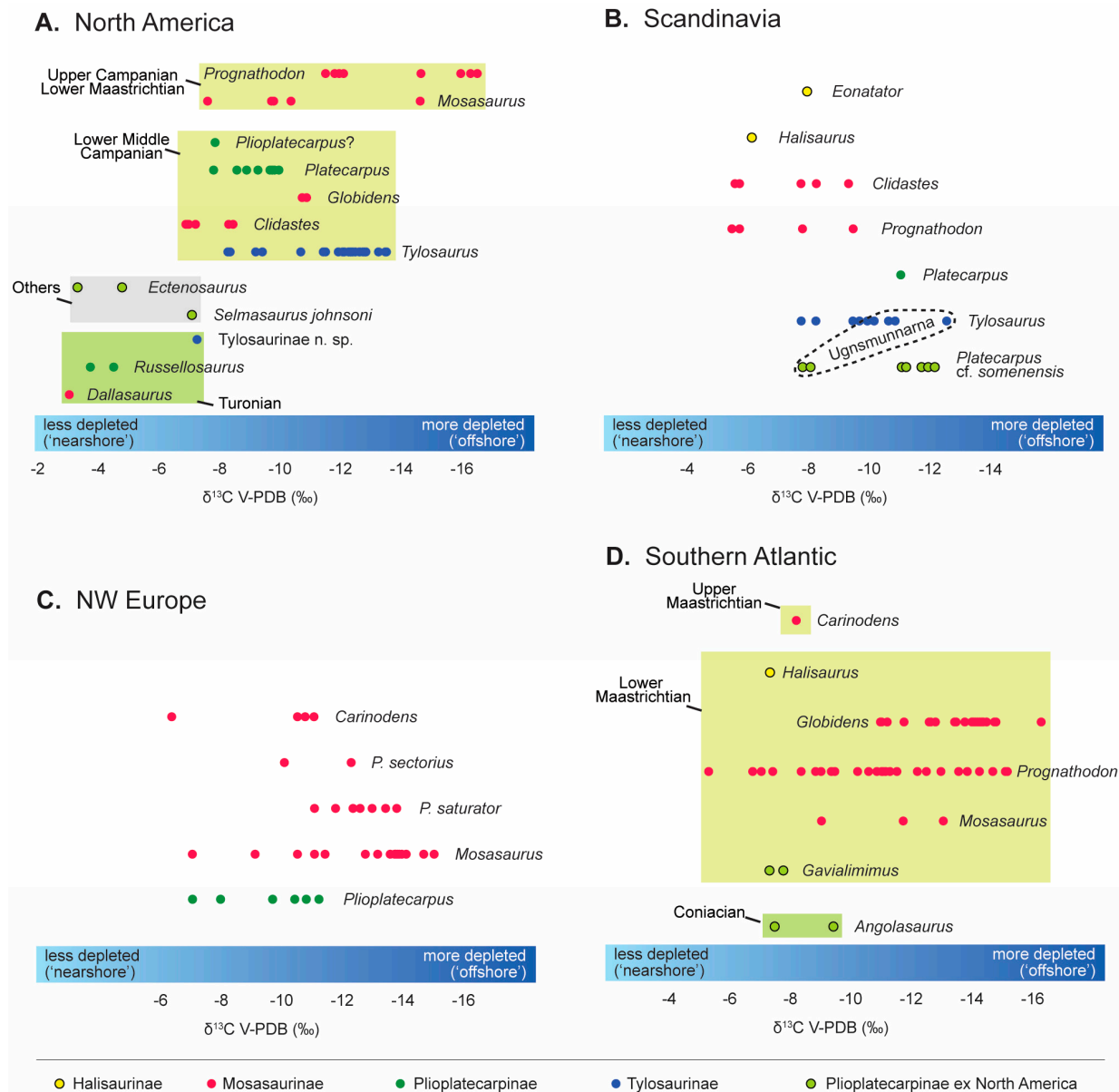


Figure 4. $\delta^{13}\text{C}$ by select geographic region. Color coding denotes subfamily membership: yellow = Halosaurinae; red = Mosasaurinae; green = Plioplatecarpinae; blue = Tylosaurinae.

For instance, the two localities from Scandinavia yielded taxonomic patterns of range occupation that differ somewhat from one another. The samples were collected from sediments at Åsen and Ugnsmunnarna, deposited at about 50 °N paleolatitude (Figure 4B). They are latest early Campanian in age (middle Campanian in the North American tripartite Campanian system) and fall within the informal *Belemnellocamax mammillatus* biozone, which is roughly 300 kyr in duration [98]. The marine succession at Åsen was deposited in a nearshore environment. The presence of floodplain sediments, hybodont shark teeth, and the topography of the adjacent basement rock (i.e., the Höljeån valley), suggest that a fluvial system was located close nearby. At Ugnsmunnarna the fauna preserves a more ontogenetically mature sample, and was likely more distal or a deeper water deposition than Åsen during the latest early Campanian [99]. The recovered $\delta^{13}\text{C}$ values range from -5.4‰ to -12.4‰ , with significant overlap among taxa; however, segregation patterns do exist. Halosaurines, with a range of values from -5.9‰ to -7.7‰ , overlap with the lowest part of the range of *Tylosaurus* (-7.6‰ to -12.4‰) and “*P.*” cf. *somenensis* (-7.6‰ to -12‰) and occupy roughly the upper half of the range of both *Clidastes* (-5.4‰ to -9.1‰)

and *Prognathodon* (−5.4‰ to −9.3‰). The relatively enriched values for the halisaurine *Eonatator* and its small body size (~3 m), suggest that this taxon was foraging in the depleted part of the Nearshore Zone. The range of values of *Clidastes* and *Prognathodon*, co-occurring in the Åsen sample, nearly overlap, suggesting that they probably occupied the same nearshore and nearshore marine foraging area, but may have been partitioning by prey size, with *Clidastes* being significantly smaller (~4 m) than the larger (~8 m) *Prognathodon* species present in the locality (e.g., [75,99]). The aggregate range of values for *Tylosaurus* and “*P.*” cf. *somenensis* largely overlap; however, the samples from Ugnsmunna occupy opposite parts of the range compared to those at Åsen (Figure 4B). It is unclear if the influence of meteoric water via river discharge at the Åsen locality had any effect on the recovered values; however, one would expect a more uniform skewing of all the taxa in the locality if this were the case. Instead, the aggregate *Tylosaurus* and *Clidastes* values are roughly comparable to the North American sample, but the nearshore Åsen sample does not contain the more depleted values for *Tylosaurus*; they are present in the more distal, offshore sample from Ugnsmunna, suggesting instead that this may be an artifact of sampling. If this is the case, the genera *Tylosaurus* and “*P.*” cf. *somenensis* co-occur in the mid-shelf to most offshore part of the range, but differences in tooth forms in those taxa (e.g., [98]) suggest possible partitioning by prey type and size.

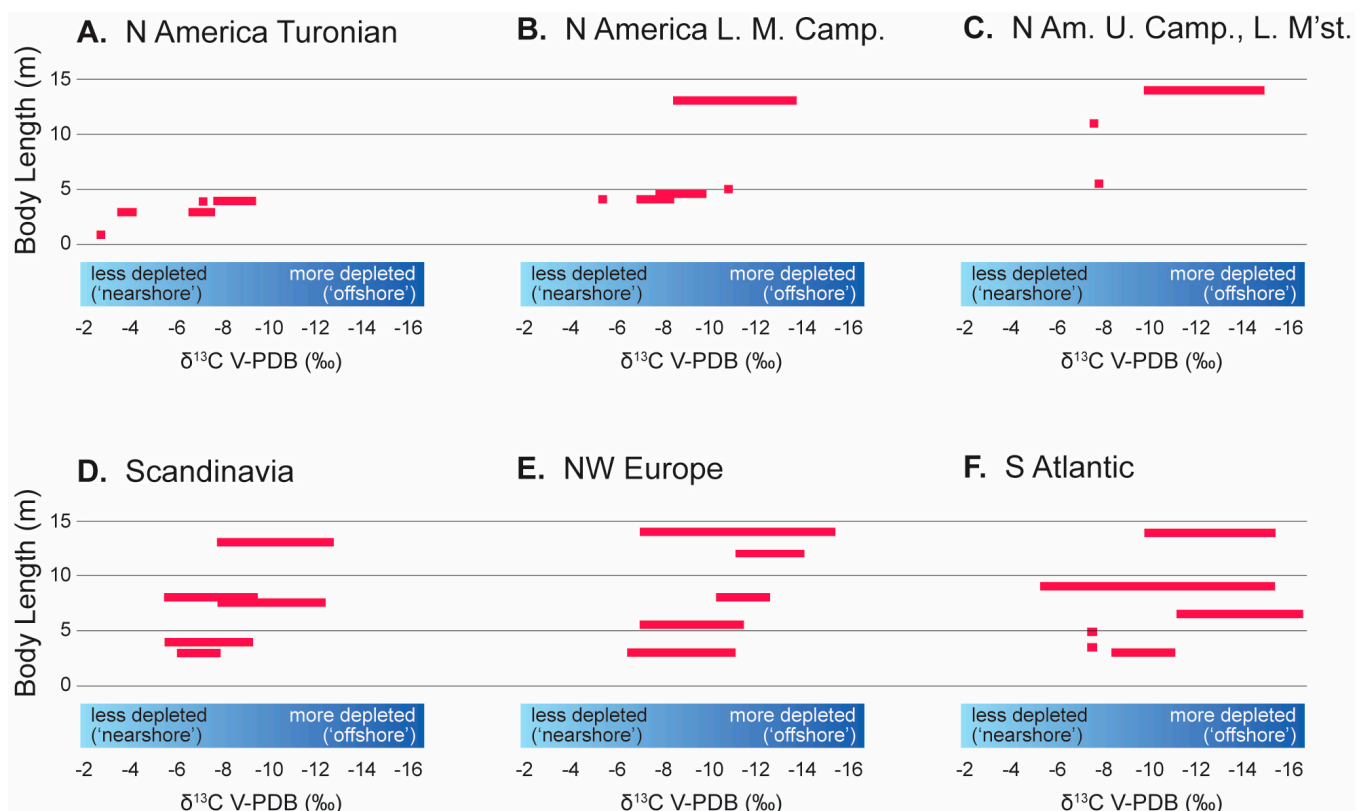


Figure 5. $\delta^{13}\text{C}$ by select geographic region and body length. Size data taken from [1].

The northeastern European sample is from the Maastrichtian type area, deposited at about 45 °N paleolatitude. Although the values at the depleted end of the range are similar to the other localities, the most enriched values (Figure 4C) are about ~2–3‰ more depleted than the other localities. Schulp et al. [37] reported isotope values for five mosasaur taxa (Figure 4C), finding that depleted $\delta^{13}\text{C}$ values largely correlate with increased body size, as previously noted by Robbins et al. [36]. With the exception of *P. saturator*, the taxa reported by [37] range through much of the Late Maastrichtian [100] and are found on a relatively shallow carbonate shelf, with water depths ranging from 80 m in the uppermost Gulpen

Formation to between 2 and 15 m in the uppermost part of the Maastricht Formation [101]. The majority of the sample (80%) is from the uppermost part of the Maastricht Formation, from relatively shallow water. As pointed out by Wendler [102], myriad variables influence the absolute values of $\delta^{13}\text{C}$ at specific localities. Thus, the more depleted values seen in the northeastern European sample, may possibly be due to local shoreline proximity and water depth, latitudinal factors, or other factors that negatively influence primary producers. This may also be the case for the *Tethysaurus* from the lower Turonian of the North African margin, which yielded relatively depleted values, incongruent with its size and level of marine adaptation. The locality that produced *Tethysaurus* was deposited in an open-platform environment [49] but under unusual and harsh conditions, indicated by a depauperate fauna [103].

Notwithstanding the large number of variables influencing primary producers [102] and the exceptions noted above, recovered $\delta^{13}\text{C}$ values with respect to body size, taxonomy, and tooth form (Figures 2–5) are largely consistent across geographies.

4.4. Evolution of Foraging Behavior in Mosasaurs

As shown above (Figure 3), early in their evolution, mosasaurs generally occupied a relatively nearshore range. Some taxonomic segregation of foraging area is already apparent between the small-bodied mosasaurines (e.g., *Dallasaurus*) and the moderately sized basal branching pliolatecarpines and tylosaurines (Figure 4). In the Coniacian–Maastrichtian, moderately sized pliolatecarpines consistently occupy the NSMZ, while both tylosaurines and mosasaurines expand their range farther offshore. Small-bodied halisaurines appear to favor a nearshore foraging area.

Dental morphology (see, e.g., [17,37,77]) broadly corresponds with the recovered $\delta^{13}\text{C}$ values. All pliolatecarpine and tylosaurine mosasaurs possess simple slightly recurved conical tooth crowns, only varying in ornamentation and robustness. A laterally compressed sectorial tooth form is first seen in early-branching mosasaurines, such as *Clidastes* in the Coniacian, and in the Campanian two new clades of mosasaurines appear: the Plotsaurini and the Globidensini (Figure 1). Globidensin mosasaurines display the most disparate range of tooth forms, suggesting a high degree of segregation by prey type and differences in feeding style, consistent with the broad range of $\delta^{13}\text{C}$ values recovered for the clade. Globidensini originates in the Campanian, evidenced by novel and diverse tooth forms, such as *Prognathodon overtoni*, which possess a robust bicarinate but squat dentition; the robust but more laterally compressed dentition of *Prognathodon* (*Dollosaurus*) *lutugini* [75,104]; and the broadly domed, durophagous dentition of *Globidens alabamaensis* [105]. By the Late Campanian, diversity in the Globidensini increases, with additional species of *Globidens* [62,106] and *Prognathodon* [107]. In the Maastrichtian, there is continued diversification, with an apparent radiation of sectorial toothed forms such as *Eremiasaurus*, *P. sectorius*, *P. kianda*, and other species previously referred to *Liodon* [63] (see also [15]). Large macrophages such as *P. saturator*, *Thalassotitan* from Morocco [17,18], and a large *Prognathodon* sp. from Angola [108] also appear in the Maastrichtian, along with durophagous forms such as the small-bodied *Carinodens* [109,110], new species of *Globidens* [73,111], and high-crowned durophages such as *Igdamanosaurus* [112] and *P. currii* [72]. Body size does not appear to correlate with foraging range in the globidensin taxa *Prognathodon kianda* and *P. lutugini*.

The range of tooth forms in globidensins stands in contrast to that of plotsaurins. A sectorial dentition is present in *Clidastes* and *Mosasaurus conodon*, while large-bodied forms such as *Mosasaurus hoffmanni* evolved a large robust macrophagous dentition and *Plotosaurus* evolved a high-aspect-ratio piscivorous (piercing) dentition. Among the plotsaurin taxa in our sample, evidence of ecological replacement occurs with the appearance

of *Mosasaurus conodon* and coincident absence of a large *Clidastes* in the upper Campanian, with which it shares a similar dentition, body size, and isotopically determined foraging range. In the Maastrichtian, the derived species *M. hoffmanni* possesses a robust tooth form and attains a large body size, both traits similar to derived *Tylosaurus* species, a taxon absent from the OSMZ in the Maastrichtian. Where foraging areas of multiple taxa overlap, apparent differences in tooth form, body size, or both occur, reflecting prey preference, suitability, or feeding niche. Foraging area occupation by multiple taxa with similar tooth forms suggests greater competition and the finer partitioning of resources.

5. Conclusions

In this contribution, we presented a large taxonomic and temporal sample of $\delta^{13}\text{C}$ values derived from tooth enamel, revealing patterns of foraging area preferences of Late Cretaceous mosasaurid squamates over evolutionary time scales (~93–66 Ma). Our results for individual localities are broadly consistent with previous studies and their predictions, but new insights were gained from the addition of the temporal axis. Notwithstanding the relatively small sample size, sparse temporal sampling for certain timeframes, and other sources of uncertainty, broad patterns of foraging segregation are apparent. Inference of foraging area preference in conjunction with other data, such as body size, tooth form, skull architecture, and swimming ability, provides the basis to evaluate niche occupation and competition over evolutionary time scales.

Patterns of foraging area segregation at the subfamily level are established early in the record, and there is a trend of increasing offshore range extension through time, broadly mirroring increases in body size in certain taxa. The nearshore foraging range, occupied by more basal forms in the Turonian, appears to be increasingly under-represented through time. Derived ruseosaurian mosasaurs are found to occupy nearshore marine and the more enriched parts of offshore marine environments, although tylosaurines achieve a large body size early and also are found to range somewhat farther offshore than plioplatecarpines. Early plioplatecarpines range from nearshore to nearshore marine areas, and the taxa with the most depleted values overlap with the earliest tylosaurines. From the Coniacian through the Maastrichtian, plioplatecarpines are largely restricted to the Nearshore Marine Zone, with a few outliers in the tribe Selmasaurini (e.g., *Selmasaurus johnsoni*, “*P.*” *somenensis*) and the plioplatecarpin genus *Ectenosaurus*. Early small-bodied mosasaurines occupy a relatively nearshore foraging area but diversify in the Campanian, and thereafter occupy the widest range of foraging areas of all the subfamilies. One mosasaurine tribe, the Globidensini, shows the greatest taxonomic diversity, plasticity of tooth form, and range of body size, and also exhibits the broadest range of isotope values of any clade. *Mosasaurus conodon* appears to replace the superficially similar, large middle Campanian *Clidastes*, and large mosasaurines (e.g., *Mosasaurus hoffmanni* and some species of *Prognathodon*) replace the large tylosaurines (*Tylosaurus*) in the upper Campanian or Lower Maastrichtian. These may be two examples of competitive exclusion as a source of extinction.

Author Contributions: Conceptualization, M.J.P., L.L.J. and J.A.R.; methodology, M.J.P. and J.A.R.; validation, M.J.P. and J.A.R.; formal analysis, M.J.P. and J.A.R.; resources, M.J.P., L.L.J., J.L. and A.S.S.; data curation, M.J.P.; writing—original draft preparation, M.J.P. and J.A.R.; visualization, M.J.P. and A.S.S.; writing—review and editing, M.J.P., L.L.J., J.L. and A.S.S. All authors have read and agreed to the published version of the manuscript.

Funding: This research received no external funding.

Data Availability Statement: Supporting data are available on request to the corresponding author.

Acknowledgments: We thank Kurt Ferguson for useful discussions and Dale Winkler for assistance with specimens in the Shuler Museum of Paleontology at SMU. We thank Chris Strganac for access to unpublished isotope data from Bentiaba, Angola, samples and Richard Zakrzewski for the permission to sample tooth enamel in the Fort Hays Sternberg Museum collection. We thank the ISEM at SMU and The Saurus Institute for their ongoing support.

Conflicts of Interest: The authors declare no conflicts of interest.

Appendix A

Table A1. The $\delta^{13}\text{C}$ values, rounded to one decimal place and listed by specimen and sample. Data sources are as follows: * = this study; [36] = Robbins et al. (2008); [37] = Schulp et al. (2013); [39] = Strganac et al. (2015); [40] = Giltaij et al. (2021); and [41] = Leuzinger et al. (2023). The Scandinavian specimens processed for this study were un-numbered specimens from the Kristianstad Basin (Sweden) collected by one of us (J.L.) and referenced in the table for this contribution as Asen1–Asen8, Kris1, Kris2, Ugn0, and Ugn1. The cell colors denote subfamily membership: yellow = Halisaurinae; red = Mosasaurinae; green = Plioplatecarpinae; and blue = Tylosaurinae. The values for $\delta^{13}\text{C}$ and $\delta^{18}\text{O}$ are represented in ‰ with respect to V-PDB, and wt.% carbonate and $\delta^{18}\text{O}$ were included for the samples for which they were available.

Specimen # (Sample #)	Taxon	Region	$\delta^{13}\text{C}$	$\delta^{18}\text{O}$	wt.% Carb *	Data Src.
Asen1 (1)	<i>Eonatator</i> sp.	Scandinavia	−7.7	−3.7	7.8	*
Asen1 (2)	<i>Eonatator</i> sp.	Scandinavia	−5.9	−2.8	7.1	*
Asen2 (1)	<i>Clidastes</i> cf. <i>C. propython</i>	Scandinavia	−9.1	−3.3	8.2	*
Asen3 (1)	<i>Clidastes</i> cf. <i>C. propython</i>	Scandinavia	−5.4	−3.1	6.4	*
Asen3 (2)	<i>Clidastes</i> cf. <i>C. propython</i>	Scandinavia	−5.4	−2.1	4.2	*
Asen3 (3)	<i>Clidastes</i> cf. <i>C. propython</i>	Scandinavia	−7.5	−2.3	4.5	*
Asen4 (1)	<i>Clidastes</i> cf. <i>C. propython</i>	Scandinavia	−8.0	-	7.8	*
SMU76391 (1)	<i>Clidastes</i> sp.	North Texas	−7.1	−3.0	5.4	[36]
SMU76391 (2)	<i>Clidastes</i> sp.	North Texas	−8.1	−3.5	4.9	[36]
SMU76404 (1)	<i>Clidastes</i> sp.	North Texas	−8.3	−3.1	3.2	[36]
SMU76281 (1)	<i>Clidastes</i> sp.	North Texas	−6.8	−3.1	5.1	[36]
SMU72184 (1)	<i>Clidastes</i> cf. <i>C. propython</i>	North Texas	−6.7	−4.3	4.6	*
SMU62504 (1)	<i>Clidastes</i> sp.	North Texas	−6.7	−3.9	4.4	*
TMM43209-1 (1)	<i>Dallasaurus turneri</i>	North Texas	−2.8	−4.4	4.8	*
MGUAN PA149 (1)	<i>Globidens phosphaticus</i>	West Africa	−13.8	−2.5	4.2	[36]
MGUAN PA149 (2)	<i>Globidens phosphaticus</i>	West Africa	−14.6	−2.3	4.4	[36]
MGUAN PA149 (3)	<i>Globidens phosphaticus</i>	West Africa	−14.0		4.5	[36]
MGUAN PA149 (4)	<i>Globidens phosphaticus</i>	West Africa	−14.0		4.8	[36]
MGUAN PA149 (5)	<i>Globidens phosphaticus</i>	West Africa	−13.9		3.2	[36]
MGUAN PA149 (6)	<i>Globidens phosphaticus</i>	West Africa	−14.1		5.0	[36]
MGUAN PA149 (7)	<i>Globidens phosphaticus</i>	West Africa	−14.0		5.9	[36]
MGUAN PA149 (8)	<i>Globidens phosphaticus</i>	West Africa	−14.1		6.0	[36]
MGUAN PA149 (9)	<i>Globidens phosphaticus</i>	West Africa	−14.2		4.0	[36]
MGUAN PA149 (10)	<i>Globidens phosphaticus</i>	West Africa	−14.1		5.8	[36]
MGUAN PA149 (11)	<i>Globidens phosphaticus</i>	West Africa	−14.0		3.0	[36]
MGUAN PA149 (12)	<i>Globidens phosphaticus</i>	West Africa	−14.0		4.4	[36]

Table A1. Cont.

Specimen # (Sample #)	Taxon	Region	$\delta^{13}\text{C}$	$\delta^{18}\text{O}$	wt.% Carb *	Data Src.
MGUAN PA149 (13)	<i>Globidens phosphaticus</i>	West Africa	−13.6		5.0	[36]
MGUAN PA149 (14)	<i>Globidens phosphaticus</i>	West Africa	−14.1		5.7	[36]
MGUAN PA149 (15)	<i>Globidens phosphaticus</i>	West Africa	−14.1		2.8	[36]
MGUAN PA149 (16)	<i>Globidens phosphaticus</i>	West Africa	−13.9		4.4	[36]
MGUAN PA149 (17)	<i>Globidens phosphaticus</i>	West Africa	−14.1		4.0	[36]
MGUAN PA149 (18)	<i>Globidens phosphaticus</i>	West Africa	−14.2		3.9	[36]
MGUAN PA149 (19)	<i>Globidens phosphaticus</i>	West Africa	−13.9		3.3	[36]
MGUAN PA149 (20)	<i>Globidens phosphaticus</i>	West Africa	−13.9		5.0	[36]
SMU76241 (1)	<i>Globidens alabamaensis</i> (juv.)	North Texas	−5.2	−2.6	4.1	[36]
SMU76241 (2)	<i>Globidens alabamaensis</i> (juv.)	North Texas	−5.3	−2.5	3.4	[36]
SMU76241 (3)	<i>Globidens alabamaensis</i> (juv.)	North Texas	−5.4	−2.6	3.7	[36]
SMU76280 (1)	<i>Globidens alabamaensis</i> (adult)	North Texas	−10.5	−3.4	3.6	[36]
SMU76280 (2)	<i>Globidens alabamaensis</i> (adult)	North Texas	−10.5	−2.2	4.3	[36]
SMU76348 (1)	<i>Mosasaurus</i> cf. <i>M. conodon</i>	North Texas	−7.4	−1.3	5.0	*
SMU76242 (1)	<i>Mosasaurus hoffmanni</i>	North Texas	−9.5	−5.3	1.0	[36]
SMU62079 (1)	<i>Prognathodon</i> sp.	North Texas	−10.1	−3.2	2.9	*
SMU76393 (1)	<i>Prognathodon kianda</i>	South Atlantic	−14.5	−2.1	4.3	[36]
SMU76393 (2)	<i>Prognathodon kianda</i>	South Atlantic	−14.9	−2.1	4.2	[36]
SMU76393 (3)	<i>Prognathodon kianda</i>	South Atlantic	−15.0	−2.0	5.0	[36]
HUJ OR 100 (1)	<i>Prognathodon currii</i>	Israel	−15.1	−2.4	3.5	*
SMU76504 (1)	<i>Prognathodon</i> cf. <i>P. overtoni</i>	North Texas	−11.3	−4.7	7.5	*
SMU76504 (2)	<i>Prognathodon</i> cf. <i>P. overtoni</i>	North Texas	−11.7	−4.5	7.5	*
Asen5 (1)	? <i>Prognathodon</i> cf. <i>P. lutugini</i>	Scandinavia	−5.4	−2.9	9.2	*
Asen5 (2)	? <i>Prognathodon</i> cf. <i>P. lutugini</i>	Scandinavia	−5.4	−2.9	8.6	*
Asen5 (3)	? <i>Prognathodon</i> cf. <i>P. lutugini</i>	Scandinavia	−7.6	−2.6	7.9	*
Asen5 (4)	? <i>Prognathodon</i> cf. <i>P. lutugini</i>	Scandinavia	−9.3	−2.4	7.6	*
SMU76503 (1)	? <i>Prognathodon</i> sp.	North Texas	−11.6	−2.3	5.4	*
SMU76503 (2)	? <i>Prognathodon</i> sp.	North Texas	−14.4	−2.2	8.1	*
SMU76503 (3)	? <i>Prognathodon</i> sp.	North Texas	−11.8	−3.4	9.1	*
SMU76503 (4)	? <i>Prognathodon</i> sp.	North Texas	−16.0	−2.6	8.4	*
SMU76503 (5)	? <i>Prognathodon</i> sp.	North Texas	−16.2	−2.7	6.6	*
SMU76503 (6)	? <i>Prognathodon</i> sp.	North Texas	−15.7	−2.6	8.4	*
SMU76334 (1)	<i>Tethysaurusnopscai</i>	North Africa	−7.5	−4.8	3.0	*
SMU76334 (2)	<i>Tethysaurusnopscai</i>	North Africa	−6.4	−3.9	2.0	*
MGUAN PA1 (1)	<i>Angolasaurus bocagei</i>	West Africa	−7.4	−0.6	3.7	*
MGUAN PA65 (1)	<i>Angolasaurus bocagei</i>	West Africa	−9.2	−2.8	4.5	*
SMU76350 (1)	<i>Ectenosaurus</i> sp.	West Texas	−3.1	−4.4	4.0	*
SMU76350 (2)	<i>Ectenosaurus</i> sp.	West Texas	−4.6	−3.0	4.0	*
FHSM VP16582 (1)	<i>Latoplatecarpus</i> sp.	Western Kansas	−7.6	−5.3	4.7	*
SMU76501 (1)	<i>Plesioplatecarpus</i> sp.	Western Kansas	−8.8	−5.8	4.8	*
Asen6 (1)	<i>Platecarpus</i> sp.	Scandinavia	−10.9		7.4	*

Table A1. Cont.

Specimen # (Sample #)	Taxon	Region	$\delta^{13}\text{C}$	$\delta^{18}\text{O}$	wt.% Carb *	Data Src.
Asen7 (1)	<i>"Platecarpus" cf. P. somenensis</i>	Scandinavia	−12.0	−4.6	8.2	*
Asen7 (2)	<i>"Platecarpus" cf. P. somenensis</i>	Scandinavia	−11.1	−4.3	8.3	*
Asen7 (3)	<i>"Platecarpus" cf. P. somenensis</i>	Scandinavia	−11.0	−2.9	8.4	*
Asen7 (4)	<i>"Platecarpus" cf. P. somenensis</i>	Scandinavia	−11.6	−4.1	7.8	*
Ugn0 (1)	<i>"Platecarpus" cf. P. somenensis</i>	Scandinavia	−7.8	−4.2	8.4	*
Ugn0 (2)	<i>"Platecarpus" cf. P. somenensis</i>	Scandinavia	−7.6	−4.1	8.4	*
SMU61617 (1)	<i>Latoplatecarpus</i> sp.	North Texas	−9.6	−4.7	6.1	*
SMU61617 (2)	<i>Latoplatecarpus</i> sp.	North Texas	−9.6	−4.4	4.8	*
SMU61617 (3)	<i>Latoplatecarpus</i> sp.	North Texas	−9.6	−3.2	5.5	*
SMU61617 (4)	<i>Latoplatecarpus</i> sp.	North Texas	−9.1	−2.8	5.4	*
SMU61617 (5)	<i>Latoplatecarpus</i> sp.	North Texas	−9.1	−4.1	5.0	*
SMU61617 (6)	<i>Latoplatecarpus</i> sp.	North Texas	−9.5	−5.1	4.9	*
SMU61617 (7)	<i>Latoplatecarpus</i> sp.	North Texas	−9.1	−3.9	4.5	*
SMU61617 (8)	<i>Latoplatecarpus</i> sp.	North Texas	−9.5	−3.6	4.9	*
SMU76381 (1)	<i>Indet. sp.</i>	North Texas	−8.4	−4.2	3.7	*
SMU76497 (1)	<i>Plesioplatecarpus</i> sp.	Texas	−7.5	−3.4	4.6	*
SMU76393 (1)	<i>Plioplatecarpus</i> sp.	Western Arkansas	−7.7	−2.8	5.4	*
SMU76498 (1)	? <i>Plioplatecarpus</i> sp.	North Texas	−7.6	−5.9	4.1	*
SMU73056 (1)	<i>Russellosaurus coheni</i>	North Texas	−4.3	−5.8	4.5	*
SMU73056 (2)	<i>Russellosaurus coheni</i>	North Texas	−3.5	−4.5	5.2	*
FHSM VP 13910 (1)	<i>Selmasaurus johnsoni</i>	Western Kansas	−6.9	−5.9	4.1	*
Asen8 (1)	<i>Tylosaurus ivoensis</i>	Scandinavia	−9.3	−3.6	6.1	*
Asen8 (2)	<i>Tylosaurus ivoensis</i>	Scandinavia	−7.6	−3.7	8.9	*
Kris1 (1)	<i>Tylosaurus ivoensis</i>	Scandinavia	−9.5	−2.5	5.9	*
Kris2 (1)	<i>Tylosaurus ivoensis</i>	Scandinavia	−8.0	−2.6	6.3	*
Ugn1 (1)	<i>Tylosaurus ivoensis</i>	Scandinavia	−12.4	−5.8	5.8	*
Ugn1 (2)	<i>Tylosaurus ivoensis</i>	Scandinavia	−10.4	−3.5	5.8	*
Ugn1 (3)	<i>Tylosaurus ivoensis</i>	Scandinavia	−9.5	−3.3	5.7	*
Ugn1 (4)	<i>Tylosaurus ivoensis</i>	Scandinavia	−9.9	−3.3	5.7	*
Ugn1 (5)	<i>Tylosaurus ivoensis</i>	Scandinavia	−10.6	−3.8	4.4	*
SMU76502 (1)	<i>Tylosaurus</i> sp.	North Texas	−8.2	−2.8	2.9	*
SMU61667 (1)	<i>Tylosaurus</i> sp.	North Texas	−8.1	−3.7	6.9	*
SMU61667 (2)	<i>Tylosaurus</i> sp.	North Texas	−9.0	−3.5	4.9	*
SMU61667 (3)	<i>Tylosaurus</i> sp.	North Texas	−10.5	−3.7	5.3	*
SMU61667 (4)	<i>Tylosaurus</i> sp.	North Texas	−11.2	−3.3	5.8	*
SMU61667 (5)	<i>Tylosaurus</i> sp.	North Texas	−11.7	−3.4	5.7	*

Table A1. Cont.

Specimen # (Sample #)	Taxon	Region	$\delta^{13}\text{C}$	$\delta^{18}\text{O}$	wt.% Carb *	Data Src.
SMU61667 (6)	<i>Tylosaurus</i> sp.	North Texas	−11.9	−4.5	6.5	*
SMU76500 (1)	<i>Tylosaurus</i> sp.	North Texas	−13.3	−6.7	3.8	*
SMU61113 (1)	<i>Tylosaurus</i> sp.	North Texas	−11.8	−3.6	5.1	*
SMU61113 (2)	<i>Tylosaurus</i> sp.	North Texas	−12.4	−3.7	6.2	*
SMU61113 (3)	<i>Tylosaurus</i> sp.	North Texas	−13.2	−4.2	5.7	*
SMU61113 (4)	<i>Tylosaurus</i> sp.	North Texas	−12.5	−4.2	6.3	*
SMU61113 (5)	<i>Tylosaurus</i> sp.	North Texas	−12.1	−3.9	5.5	*
SMU61113 (6)	<i>Tylosaurus</i> sp.	North Texas	−12.1	−4.9	6.3	*
SMU61113 (7)	<i>Tylosaurus</i> sp.	North Texas	−12.1	−3.5	4.4	*
SMU61113 (8)	<i>Tylosaurus</i> sp.	North Texas	−12.6	−3.1	5.1	*
SMU61113 (9)	<i>Tylosaurus</i> sp.	North Texas	−12.1	−2.9	4.9	*
SMU76392 (1)	<i>Tylosaurus</i> sp.	North Texas	−13.0	−5.8	5.4	*
SMU76392 (2)	<i>Tylosaurus</i> sp.	North Texas	−12.6	−4.5	4.1	*
SMU76392 (3)	<i>Tylosaurus</i> sp.	North Texas	−12.5	−6.1	5.6	*
SMU76392 (4)	<i>Tylosaurus</i> sp.	North Texas	−12.5	−4.8	4.3	*
SMU76392 (5)	<i>Tylosaurus</i> sp.	North Texas	−12.2	−4.2	4.5	*
LO7786 (1)	<i>Tylosaurus</i> sp.	North Texas	−7.0	−4.8	6.7	*
SMU75374 (1)	<i>Tylosaurus</i> sp.	North Texas	−11.7	−6.2	6.3	*
SMU75374 (2)	<i>Tylosaurus</i> sp.	North Texas	−11.2	−6.3	5.9	*
SMU75374 (3)	<i>Tylosaurus</i> sp.	North Texas	−11.8	−6.9	6.8	*
SMU75374 (4)	<i>Tylosaurus</i> sp.	North Texas	−12.0	−6.2	5.3	*
SMU76382 (1)	<i>Tylosaurus</i> sp.	North Texas	−9.2	−4.2	2.	*
SMU75586 (1)	<i>Tylosaurus</i> sp.	North Texas	−10.3		8.2	*
NHMM 1980.6 (1)	<i>Carinodensbelgicus</i>	Northern Europe	−10.8	−4.0		[37]
NHMM 1980.7 (1)	<i>Carinodensbelgicus</i>	Northern Europe	−10.5	−2.3		[37]
NHMM 1980.7 (2)	<i>Carinodensbelgicus</i>	Northern Europe	−10.5	−2.3		[37]
NHMM 7354 (1)	<i>Carinodensbelgicus</i>	Northern Europe	−10.3	−3.6		[37]
NHMM 1984.88.1A (1)	<i>Plioplatecarpusmarshi</i>	Northern Europe	−10.7	−4.5		[37]
NHMM 1984.88.1A (2)	<i>Plioplatecarpusmarshi</i>	Northern Europe	−11.1	−4.5		[37]
NHMM 1984.88.1B	<i>Plioplatecarpusmarshi</i>	Northern Europe	−10.3			[37]
NHMM 1995 031 (1)	<i>Prognathodon sectorius</i>	Northern Europe	−9.9	−3.4		[37]
NHMM LV 150 (1)	<i>Prognathodon sectorius</i>	Northern Europe	−12.2	−3.0		[37]
NHMM 1998 141 (1)	<i>Prognathodonsaturator</i>	Northern Europe	−12.8			[37]
NHMM 1998 141 (2)	<i>Prognathodonsaturator</i>	Northern Europe	−13.3	−3.4		[37]
NHMM 1998 141 (3)	<i>Prognathodonsaturator</i>	Northern Europe	−13.6	−3.0		[37]
NHMM 1998 141 (4)	<i>Prognathodonsaturator</i>	Northern Europe	−12.3	−2.8		[37]
NHMM 1998 141 (5)	<i>Prognathodonsaturator</i>	Northern Europe	−12.3	−3.1		[37]
NHMM 1317.02 (1)	<i>Mosasaurushoffmanni</i>	Northern Europe	−9.3	−3.2		[37]
NHMM MK 591 (1)	<i>Mosasaurushoffmanni</i>	Northern Europe	−7.1			[37]
NHMM 4560 (1)	<i>Mosasaurushoffmanni</i>	Northern Europe	−11.3	−3.8		[37]
NHMM 1446 (1)	<i>Mosasaurushoffmanni</i>	Northern Europe	−13.7			[37]

Table A1. Cont.

Specimen # (Sample #)	Taxon	Region	$\delta^{13}\text{C}$	$\delta^{18}\text{O}$	wt.% Carb *	Data Src.
NHMM 1446 (2)	<i>Mosasaurushoffmanni</i>	Northern Europe	−13.0	−4.4		[37]
NHMM 1446 (3)	<i>Mosasaurushoffmanni</i>	Northern Europe	−12.6	−4.0		[37]
NHMM 1446 (4)	<i>Mosasaurushoffmanni</i>	Northern Europe	−13.8	−6.2		[37]
NHMM 1446 (5)	<i>Mosasaurushoffmanni</i>	Northern Europe	−14.0	−4.4		[37]
NHMM 1446 (6)	<i>Mosasaurushoffmanni</i>	Northern Europe	−13.4	−5.3		[37]
NHMM 1446 (7)	<i>Mosasaurushoffmanni</i>	Northern Europe	−13.6	−4.0		[37]
NHMM 1446 (8)	<i>Mosasaurushoffmanni</i>	Northern Europe	−14.9	−3.9		[37]
NHMM 1446 (9)	<i>Mosasaurushoffmanni</i>	Northern Europe	−14.5	−3.9		[37]
NHMM 1446 (10)	<i>Mosasaurushoffmanni</i>	Northern Europe	−13.7	−3.8		[37]
NHMM 1446 (11)	<i>Mosasaurushoffmanni</i>	Northern Europe	−13.6	−6.2		[37]
MGUAN PA 171 (1)	<i>Carinodens</i> sp.	West Africa	−8.1	−1.5		[39]
MGUAN PA 04 (1)	<i>Globidens phosphaticus</i>	West Africa	−14.6	−2.1		[39]
MGUAN PA 05 (1)	<i>Globidens phosphaticus</i>	West Africa	−13.2	−1.7		[39]
MGUAN PA 29 (1)	<i>Globidens phosphaticus</i>	West Africa	−14.3	−1.2		[39]
MGUAN PA 30 (1)	<i>Globidens phosphaticus</i>	West Africa	−10.8	−1.3		[39]
MGUAN PA 301 (1)	<i>Globidens phosphaticus</i>	West Africa	−12.6	−1.1		[39]
MGUAN PA 307 (1)	<i>Globidens phosphaticus</i>	West Africa	−11.6	−1.7		[39]
MGUAN PA 31 (1)	<i>Globidens phosphaticus</i>	West Africa	−12.4	−1.1		[39]
MGUAN PA 313 (1)	<i>Globidens phosphaticus</i>	West Africa	−12.5	−1.5		[39]
MGUAN PA 33 (1)	<i>Globidens phosphaticus</i>	West Africa	−11.0	−2.4		[39]
MGUAN PA 500 (1)	<i>Globidens phosphaticus</i>	West Africa	−16.1	−2.1		[39]
MGUAN PA 61 (1)	<i>Globidens phosphaticus</i>	West Africa	−14.3	−1.6		[39]
MGUAN PA 314 (1)	<i>Halisaurus</i> sp.	West Africa	−7.2	−2.2		[39]
MGUAN PA 309 (1)	<i>Mosasaurus</i> sp.	West Africa	−11.6	−1.4		[39]
MGUAN PA 309 (2)	<i>Mosasaurus</i> sp.	West Africa	−8.9	−1.4		[39]
MGUAN PA 44 (1)	<i>Mosasaurus</i> sp.	West Africa	−11.6	−2.6		[39]
MGUAN PA 46 (1)	<i>Mosasaurus</i> sp.	West Africa	−12.9	−1.9		[39]
MGUAN PA 177 (1)	<i>Gavialimimus</i> sp.	West Africa	−7.2	−2.1		[39]
MGUAN PA 312 (1)	<i>Gavialimimus</i> sp.	West Africa	−7.2	−2.1		[39]
MGUAN PA 312 (2)	<i>Gavialimimus</i> sp.	West Africa	−7.6	−2.4		[39]
MGUAN PA 525 (1)	<i>Gavialimimus</i> sp.	West Africa	−9.2	−2.6		[39]
MGUAN PA 525 (2)	<i>Gavialimimus</i> sp.	West Africa	−9.2	−3.3		[39]
MGUAN PA 321 (1)	<i>Gavialimimus</i> sp.	West Africa	−8.2	−2.3		[39]
MGUAN PA 38 (1)	<i>Gavialimimus</i> sp.	West Africa	−10.9	−1.5		[39]
MGUAN PA 55 (1)	<i>Gavialimimus</i> sp.	West Africa	−8.7	−3.6		[39]
MGUAN PA528 (1)	<i>Prognathodon kianda</i>	West Africa	−8.9	−1.4		[39]
MGUAN PA 526 (1)	<i>Prognathodon kianda</i>	West Africa	−9.3	−1.9		[39]
MGUAN PA 527 (1)	<i>Prognathodon kianda</i>	West Africa	−9.2	−2.3		[39]
MGUAN PA 28 (2)	<i>Prognathodon kianda</i>	West Africa	−11.1	−1.6		[39]
MGUAN PA 28 (1)	<i>Prognathodon kianda</i>	West Africa	−11.4	−2.3		[39]
MGUAN PA 304 (1)	<i>Prognathodon kianda</i>	West Africa	−7.3	−1.5		[39]
MGUAN PA 304 (2)	<i>Prognathodon kianda</i>	West Africa	−6.9	−1.6		[39]

Table A1. Cont.

Specimen # (Sample #)	Taxon	Region	$\delta^{13}\text{C}$	$\delta^{18}\text{O}$	wt.% Carb *	Data Src.
MGUAN PA 306 (1)	<i>Prognathodon kianda</i>	West Africa	−12.1	−2.4		[39]
MGUAN PA 315 (1)	<i>Prognathodon kianda</i>	West Africa	−10.1	−1.8		[39]
MGUAN PA 318 (1)	<i>Prognathodon kianda</i>	West Africa	−12.4	−2.4		[39]
MGUAN PA 35 (1)	<i>Prognathodon kianda</i>	West Africa	−10.7	−1.5		[39]
MGUAN PA 40 (1)	<i>Prognathodon kianda</i>	West Africa	−11.0	−1.7		[39]
MGUAN PA 41 (1)	<i>Prognathodon kianda</i>	West Africa	−5.2	−1.9		[39]
MGUAN PA 45 (1)	<i>Prognathodon kianda</i>	West Africa	−10.4	−3.3		[39]
MGUAN PA 47 (1)	<i>Prognathodon kianda</i>	West Africa	−13.7	−2.4		[39]
MGUAN PA 48 (1)	<i>Prognathodon kianda</i>	West Africa	−10.9	−1.6		[39]
MGUAN PA 50 (1)	<i>Prognathodon kianda</i>	West Africa	−14.1	−3.7		[39]
MGUAN PA 50 (2)	<i>Prognathodon kianda</i>	West Africa	−13.4	−1.9		[39]
MGUAN PA 53 (1)	<i>Prognathodon kianda</i>	West Africa	−12.8	−3.5		[39]
MGUAN PA 56 (1)	<i>Prognathodon kianda</i>	West Africa	−6.6	−2.0		[39]
NHMD 157504 (1)	<i>Carinodensminalmamar</i>	Scandinavia	−6.3	−3.1		[40]
NHMD 227349 (1)	<i>Mosasaurus</i> sp.	Scandinavia	−11.1	−2.5		[40]
OESM 8783 (1)	<i>Mosasaurus</i> sp.	Scandinavia	−8.6	−2.6		[40]
NHMM 1984089-1 (1)	<i>Mosasaurushoffmanni</i>	Northern Europe	−10.3	−2.7		[40]
NHMM 1984089-1 (2)	<i>Mosasaurushoffmanni</i>	Northern Europe	−9.0	−3.4		[40]
NHMD 226499 (1)	<i>Mosasaurus</i> cf. <i>M. hoffmanni</i>	Scandinavia	−6.9	−2.8		[40]
NHMD 226499 (2)	<i>Mosasaurus</i> cf. <i>M. hoffmanni</i>	Scandinavia	−11.0	−2.7		[40]
NHMD 227350 (1)	<i>Plioplatecarpus</i> sp.	Scandinavia	0.2	−3.4		[40]
NHMD 189763 (1)	<i>Plioplatecarpus</i> sp.	Scandinavia	−9.5	−2.8		[40]
NHMM 1997289 (1)	<i>Plioplatecarpusmarshi</i>	Northern Europe	−7.0	−2.4		[40]
NHMM 1997289 (2)	<i>Plioplatecarpusmarshi</i>	Northern Europe	−7.9	−4.0		[40]
NHMM 1998141-11 (1)	<i>Prognathodonsaturator</i>	Northern Europe	−10.9	−2.7		[40]
NHMM 1998141-7 (1)	<i>Prognathodonsaturator</i>	Northern Europe	−11.6	−2.5		[40]
MLP 15-I-24-41a: ARG-1 (1)	<i>Mosasauridae</i> indet.	Antarctica	−8.2	−4.0		[41]
MLP 15-I-24-44: ARG-3 (1)	<i>Globidensini</i> indet.	Antarctica	−11.2	−4.6		[41]
MLP 15-I-24-48: ARG-4 (1)	? <i>Mosasaurus</i> indet.	Antarctica	−11.8	−4.4		[41]
MLP 15-I-24-33a: ARG-5 (1)	cf. <i>Liodon</i> indet.	Antarctica	−13.5	−3.9		[41]
MLP 15-I-24-33a: ARG-5 (2)	cf. <i>Liodon</i> indet.	Antarctica	−11.4	−3.6		[41]
MLP 15-I-24-29: ARG-8 (1)	? <i>Taniwhasaurus</i> indet.	Antarctica	−10.6	−4.8		[41]
MLP 15-I-24-55a: ARG-10 (1)	? <i>Taniwhasaurus</i> indet.	Antarctica	−6.8	−4.8		[41]
MLP 15-I-24-25: ARG-13 (1)	cf. <i>Liodon</i> indet.	Antarctica	−11.8	−3.5		[41]

Table A1. Cont.

Specimen # (Sample #)	Taxon	Region	$\delta^{13}\text{C}$	$\delta^{18}\text{O}$	wt.% Carb *	Data Src.
MLP 15-I-24-33b: ARG-14 (1)	cf. <i>Liodon</i> indet.	Antarctica	−12.5	−2.6		[41]
MLP 13-XI-19-38: ARG-18 (1)	? <i>Mosasaurinae</i> indet.	Argentina	−11.1	−5.1		[41]
MLP 13-XI-19-38: ARG-19	? <i>Mosasaurinae</i> indet.	Argentina	−11.1	−4.2		[41]

References

- Polcyn, M.J.; Jacobs, L.L.; Araújo, R.; Schulp, A.S.; Mateus, O. Physical Drivers of Mosasaur Evolution. *Palaeogeogr. Palaeoclimatol. Palaeoecol.* **2014**, *400*, 17–27. [\[CrossRef\]](#)
- Augusta, B.G.; Zaher, H.; Polcyn, M.J.; Fiorillo, A.R.; Jacobs, L.L. A Review of Non-Mosasaurid (Dolichosaur and Aigialosaur) Mosasaurs and Their Relationships to Snakes. In *The Origin and Early Evolutionary History of Snakes*; Gower, D.J., Zaher, H., Eds.; Systematics Association Special Volume Series; Cambridge University Press: Cambridge, UK, 2022; pp. 157–179, ISBN 978-1-108-93889-1.
- Lindgren, J.; Polcyn, M.J.; Young, B.A. Landlubbers to Leviathans: Evolution of Swimming in Mosasaurine Mosasaurs. *Paleobiology* **2011**, *37*, 445–469. [\[CrossRef\]](#)
- Dollo, L. Le Hainosaure et Les Nouveaux Vertébrés Fossiles Du Musée de Bruxelles. *Rev. Des. Quest. Sci.* **1887**, *21*, 504–539.
- Williston, S. Some Additional Characters of the Mosasaurs. *Kans. Univ. Q.* **1899**, *8*, 39–41.
- Sternberg, C.H. Explorations of the Permian of Texas and the Chalk of Kansas, 1918. *Trans. Kans. Acad. Sci.* **1919**, *30*, 119–120. [\[CrossRef\]](#)
- Camp, C.L. California Mosasaurs. *Mem. Univ. Calif.* **1942**, *13*, 1.
- Massare, J.A. Tooth Morphology and Prey Preference of Mesozoic Marine Reptiles. *J. Vertebr. Paleontol.* **1987**, *7*, 121–137. [\[CrossRef\]](#)
- Martin, J.E.; Bjork, P.P. Gastric Residues Associated with a Mosasaur from the Late Cretaceous (Campanian) Pierre Shale in South Dakota. In *Papers in Vertebrate Paleontology in Honor of Morton Green*; Martin, J.E., Ostrander, G.E., Eds.; Dakoterra; South Dakota School of Mines & Technology: Rapid City, SD, USA, 1987.
- Everhart, M. Plesiosaurs as the Food of Mosasaurs; New Data on the Stomach Contents of a *Tylosaurus proriger* (Squamata; Mosasauridae) from the Niobrara Formation of Western Kansas. *Mosasaur* **2004**, *7*, 41–46.
- Schulp, A.S. Feeding the Mechanical Mosasaur: What Did *Carinodens* Eat? *Neth. J. Geosci.* **2005**, *84*, 345–357. [\[CrossRef\]](#)
- Martin, J.E.; Fox, J.E. Stomach Contents of *Globidens*, a Shell-Crushing Mosasaur (Squamata), from the Late Cretaceous Pierre Shale Group, Big Bend Area of the Missouri River, Central South Dakota. In *The Geology and Paleontology of the Late Cretaceous Marine Deposits of the Dakotas*; Martin, J.E., Paris, D., Eds.; Geological Society of America Special Papers; Geological Society of America: Boulder, CO, USA, 2007; Volume 427, pp. 167–176.
- Einarsson, E.; Lindgren, J.; Kear, B.P.; Siverson, M. Mosasaur Bite Marks on a Plesiosaur Propodial from the Campanian (Late Cretaceous) of Southern Sweden. *GFF* **2010**, *132*, 123–128. [\[CrossRef\]](#)
- Poynter, J.M. Using Dental Microwear Analysis to Predict Feeding Types in Mesozoic Marine Reptiles. Ph.D. Thesis, Northwest Missouri State University, Maryville, MO, USA, 2011.
- Konishi, T.; Brinkman, D.; Massare, J.A.; Caldwell, M.W. New Exceptional Specimens of *Prognathodon overtoni* (Squamata, Mosasauridae) from the Upper Campanian of Alberta, Canada, and the Systematics and Ecology of the Genus. *J. Vertebr. Paleontol.* **2011**, *31*, 1026–1046. [\[CrossRef\]](#)
- Konishi, T.; Newbrey, M.G.; Caldwell, M.W. A Small, Exquisitely Preserved Specimen of *Mosasaurus missouriensis* (Squamata, Mosasauridae) from the Upper Campanian of the Bearpaw Formation, Western Canada, and the First Stomach Contents for the Genus. *J. Vertebr. Paleontol.* **2014**, *34*, 802–819. [\[CrossRef\]](#)
- Bardet, N.; Houssaye, A.; Vincent, P.; Pereda Suberbiola, X.; Amaghazaz, M.; Jourani, E.; Meslouh, S. Mosasaurs (Squamata) from the Maastrichtian Phosphates of Morocco: Biodiversity, Palaeobiogeography and Palaeoecology Based on Tooth Morphoguilds. *Gondwana Res.* **2015**, *27*, 1068–1078. [\[CrossRef\]](#)
- Longrich, N.R.; Jalil, N.-E.; Khaldoune, F.; Yazami, O.K.; Pereda-Suberbiola, X.; Bardet, N. *Thalassotitan atrox*, a Giant Predatory Mosasaurid (Squamata) from the Upper Maastrichtian Phosphates of Morocco. *Cretac. Res.* **2022**, *140*, 105315. [\[CrossRef\]](#)
- Holwerda, F.M.; Bestwick, J.; Purnell, M.A.; Jagt, J.W.M.; Schulp, A.S. Three-Dimensional Dental Microwear in Type-Maastrichtian Mosasaur Teeth (Reptilia, Squamata). *Sci. Rep.* **2023**, *13*, 18720. [\[CrossRef\]](#)

20. Polcyn, M.J.; Schulp, A.S.; Goncalves, A.O. Remarkably Well-Preserved in-Situ Gut-Content in a Specimen of *Prognathodon kianda* (Squamata: Mosasauridae) Reveals Multispecies Intrafamilial Predation, Cannibalism, and a New Mosasaurine Taxon. In *Windows into Sauropsid and Synapsid Evolution*; Lee, Y.-N., Ed.; Dinosaur Science Center Press: Hwaseong City, Republic of Korea, 2023; pp. 66–98.
21. Russell, D.A. *Systematics and Morphology of American Mosasaurs*; Yale University Press: New Haven, CT, USA, 1967; ISBN 978-1-933789-45-3.
22. Holmes, R.; Caldwell, M.W.; Cumbaa, S.L. A New Specimen of *Plioplatecarpus* (Mosasauridae) from the Lower Maastrichtian of Alberta: Comments on Allometry, Functional Morphology, and Paleocology. *Can. J. Earth Sci.* **1999**, *36*, 363–369. [\[CrossRef\]](#)
23. Kiernan, C.R. Stratigraphic Distribution and Habitat Segregation of Mosasaurs in the Upper Cretaceous of Western and Central Alabama, with an Historical Review of Alabama Mosasaur Discoveries. *J. Vertebr. Paleontol.* **2002**, *22*, 91–103. [\[CrossRef\]](#)
24. Nicholls, E.L.; Meckert, D. Marine Reptiles from the Nanaimo Group (Upper Cretaceous) of Vancouver Island. *Can. J. Earth Sci.* **2002**, *39*, 1591–1603. [\[CrossRef\]](#)
25. Jacobs, L.L.; Polcyn, M.J.; Taylor, L.H.; Ferguson, K. Sea-Surface Temperatures and Palaeoenvironments of Dolichosaurs and Early Mosasaurs. *Geol. Mijnb.* **2005**, *84*, 269–281. [\[CrossRef\]](#)
26. Ifrim, C.; Stinnesbeck, W.; Frey, E. Upper Cretaceous (Cenomanian-Turonian and Turonian-Coniacian) Open Marine Plattenkalk Deposits in NE Mexico. *Neues Jahrb. Für Geol. Und Paläontologie Abh.* **2007**, *245*, 71–81. [\[CrossRef\]](#)
27. Patrick, D.; Martin, J.; Parris, D.; Grandstaff, D. Paleoenvironmental Interpretations of Rare Earth Element Signatures in Mosasaurs (Reptilia) from the Upper Cretaceous Pierre Shale, Central South Dakota, USA. *Palaeogeogr. Palaeoclimatol. Palaeoecol.* **2004**, *212*, 277–294. [\[CrossRef\]](#)
28. Kocsis, L.; Ősi, A.; Vennemann, T.; Trueman, C.N.; Palmer, M.R. Geochemical Study of Vertebrate Fossils from the Upper Cretaceous (Santonian) Csehbánya Formation (Hungary): Evidence for a Freshwater Habitat of Mosasaurs and Pycnodont Fish. *Palaeogeogr. Palaeoclimatol. Palaeoecol.* **2009**, *280*, 532–542. [\[CrossRef\]](#)
29. Harrell, T.L.; Pérez-Huerta, A. Habitat Preference of Mosasaurs Indicated by Rare Earth Element (REE) Content of Fossils from the Upper Cretaceous Marine Deposits of Alabama, New Jersey, and South Dakota (USA). *Neth. J. Geosci.* **2015**, *94*, 145–154. [\[CrossRef\]](#)
30. Reisdorf, A.G.; Bux, R.; Wyler, D.; Benecke, M.; Klug, C.; Maisch, M.W.; Fornaro, P.; Wetzel, A. Float, Explode or Sink: Postmortem Fate of Lung-Breathing Marine Vertebrates. *Palaeobiodivers. Palaeoenviron.* **2012**, *92*, 67–81. [\[CrossRef\]](#)
31. DeNiro, M.J.; Epstein, S. Influence of Diet on the Distribution of Carbon Isotopes in Animals. *Geochim. Cosmochim. Acta* **1978**, *42*, 495–506. [\[CrossRef\]](#)
32. Clementz, M.T.; Koch, P.L. Differentiating Aquatic Mammal Habitat and Foraging Ecology with Stable Isotopes in Tooth Enamel. *Oecologia* **2001**, *129*, 461–472. [\[CrossRef\]](#)
33. Fry, B.; Wainright, S.C. Diatom Sources of ^{13}C -Rich Carbon in Marine Food Webs. *Mar. Ecol. Prog. Ser.* **1991**, *76*, 149–157. [\[CrossRef\]](#)
34. Rau, G.H.; Takahashi, T.; Des Marais, D.J.; Repeta, D.J.; Martin, J.H. The Relationship between $\delta^{13}\text{C}$ of Organic Matter and $[\text{CO}_2(\text{Aq})]$ in Ocean Surface Water: Data from a JGOFS Site in the Northeast Atlantic Ocean and a Model. *Geochim. Cosmochim. Acta* **1992**, *56*, 1413–1419. [\[CrossRef\]](#)
35. Hemminga, M.; Mateo, M. Stable Carbon Isotopes in Seagrasses: Variability in Ratios and Use in Ecological Studies. *Mar. Ecol. Prog. Ser.* **1996**, *140*, 285–298. [\[CrossRef\]](#)
36. Robbins, J.; Ferguson, K.M.; Polcyn, M.J.; Jacobs, L.L. Application of Stable Carbon Isotope Analysis to Mosasaur Ecology. In *Proceedings of the Second Mosasaur Meeting*; Everhart, M.J., Ed.; Sternberg Museum of Natural History, Fort Hays State University: Hays, KS, USA, 2008; Volume Special Volume; pp. 123–130, ISBN 978-0-615-23109-9.
37. Schulp, A.S.; Vonhof, H.B.; Van Der Lubbe, J.H.J.L.; Janssen, R.; Van Baal, R.R. On Diving and Diet: Resource Partitioning in Type-Maastrichtian Mosasaurs. *Neth. J. Geosci.* **2013**, *92*, 165–170. [\[CrossRef\]](#)
38. Schulp, A.S.; Janssen, R.; Van Baal, R.R.; Jagt, J.W.M.; Mulder, E.W.A.; Vonhof, H.B. Stable Isotopes, Niche Partitioning and the Paucity of Elasmosaur Remains in the Maastrichtian Type Area. *Neth. J. Geosci.* **2017**, *96*, 29–33. [\[CrossRef\]](#)
39. Strganac, C.; Jacobs, L.L.; Polcyn, M.J.; Mateus, O.; Myers, T.S.; Salminen, J.; May, S.R.; Araújo, R.; Ferguson, K.M.; Gonçalves, A.O.; et al. Geological Setting and Paleocology of the Upper Cretaceous Bench 19 Marine Vertebrate Bonebed at Bentiaba, Angola. *Neth. J. Geosci.* **2015**, *94*, 121–136. [\[CrossRef\]](#)
40. Giltaij, T.J.; Jeroen, V.D.L.; Lindow, B.; Schulp, A.S.; Jagt, J.W.M. Carbon Isotope Trends in North-West European Mosasaurs (Squamata; Late Cretaceous). *Bull. Geol. Soc. Den.* **2021**, *69*, 59–70. [\[CrossRef\]](#)
41. Leuzinger, L.; Kocsis, L.; Luz, Z.; Vennemann, T.; Ulyanov, A.; Fernández, M. Latest Maastrichtian Middle- and High-Latitude Mosasaurs and Fish Isotopic Composition: Carbon Source, Thermoregulation Strategy, and Thermal Latitudinal Gradient. *Paleobiology* **2023**, *49*, 353–373. [\[CrossRef\]](#)

42. Strong, C.R.C.; Caldwell, M.W.; Konishi, T.; Palci, A. A New Species of Longirostrine Plioplatecarpine Mosasaur (Squamata: Mosasauridae) from the Late Cretaceous of Morocco, with a Re-Evaluation of the Problematic Taxon ‘*Platecarpus*’ *ptychodon*. *J. Syst. Palaeontol.* **2020**, *18*, 1769–1804. [\[CrossRef\]](#)
43. Polcyn, M.J.; Bardet, N.; Albright, L.B.; Titus, A. A New Lower Turonian Mosasaurid from the Western Interior Seaway and the Antiquity of the Unique Basicranial Circulation Pattern in Plioplatecarpinae. *Cretac. Res.* **2023**, *151*, 105621. [\[CrossRef\]](#)
44. Zietlow, A.R.; Boyd, C.A.; Van Vranken, N.E. *Jormungandr walhallaensis*: A New Mosasaurine (Squamata: Mosasauroida) from the Pierre Shale Formation (Pembina Member: Middle Campanian) of North Dakota. *Bull. Am. Mus. Nat. Hist.* **2023**, *464*, 1–82. [\[CrossRef\]](#)
45. Longrich, N.R.; Polcyn, M.J.; Jalil, N.-E.; Pereda-Suberbiola, X.; Bardet, N. A Bizarre New Plioplatecarpine Mosasaurid from the Maastrichtian of Morocco. *Cretac. Res.* **2024**, *160*, 105870. [\[CrossRef\]](#)
46. Polcyn, M.J.; Bell, G.L., Jr.; Shimada, K.; Everhart, M.J. The Oldest North American Mosasaurs (Squamata: Mosasauridae) from the Turonian (Upper Cretaceous) of Kansas and Texas with Comments on the Radiations of Major Mosasaur Clades. In *Proceedings of the Second Mosasaur Meeting*; Everhart, M.J., Ed.; Sternberg Museum of Natural History, Fort Hays State University: Hays, KS, USA, 2008; Volume Special Volume; pp. 137–155, ISBN 978-0-615-23109-9.
47. Bell, G.L. A Phylogenetic Revision of North American and Adriatic Mosasauroida. In *Ancient Marine Reptiles*; Elsevier: Amsterdam, The Netherlands, 1997; pp. 293–332, ISBN 978-0-12-155210-7.
48. Páramo-Fonseca, M.E. *Yaguarasaurus columbianus* (Reptilia, Mosasauridae), a Primitive Mosasaur from the Turonian (Upper Cretaceous) of Colombia. *Hist. Biol.* **2000**, *14*, 121–131. [\[CrossRef\]](#)
49. Bardet, N.; Suberbiola, X.P.; Jalil, N.-E. A New Mosasauroid (Squamata) from the Late Cretaceous (Turonian) of Morocco. *Comptes Rendus Palevol* **2003**, *2*, 607–616. [\[CrossRef\]](#)
50. Polcyn, M.J.; Bell, G.L. *Russellosaurus coheni* n. gen., n. sp., a 92 Million-Year-Old Mosasaur from Texas (USA), and the Definition of the Parafamily Russellosaurina. *Neth. J. Geosci.* **2005**, *84*, 321–333. [\[CrossRef\]](#)
51. Polcyn, M.J.; Everhart, M.J. Description and Phylogenetic Analysis of a New Species of *Selmasaurus* (Mosasauridae: Plioplatecarpinae) from the Niobrara Chalk of Western Kansas. In *Proceedings of the Second Mosasaur Meeting*; Everhart, M.J., Ed.; Sternberg Museum of Natural History, Fort Hays State University: Hays, KS, USA, 2008; Volume Special Volume; pp. 13–28, ISBN 978-0-615-23109-9.
52. Konishi, T.; Caldwell, M.W. Two New Plioplatecarpine (Squamata, Mosasauridae) Genera from the Upper Cretaceous of North America, and a Global Phylogenetic Analysis of Plioplatecarpines. *J. Vertebr. Paleontol.* **2011**, *31*, 754–783. [\[CrossRef\]](#)
53. Leblanc, A.R.H.; Caldwell, M.W.; Bardet, N. A New Mosasaurine from the Maastrichtian (Upper Cretaceous) Phosphates of Morocco and Its Implications for Mosasaurine Systematics. *J. Vertebr. Paleontol.* **2012**, *32*, 82–104. [\[CrossRef\]](#)
54. Palci, A.; Caldwell, M.W.; Papazzoni, C.A. A New Genus and Subfamily of Mosasaurs from the Upper Cretaceous of Northern Italy. *J. Vertebr. Paleontol.* **2013**, *33*, 599–612. [\[CrossRef\]](#)
55. Willman, A.J.; Konishi, T.; Caldwell, M.W. A New Species of *Ectenosaurus* (Mosasauridae: Plioplatecarpinae) from Western Kansas, USA, Reveals a Novel Suite of Osteological Characters for the Genus¹. *Can. J. Earth Sci.* **2021**, *58*, 741–755. [\[CrossRef\]](#)
56. Kiernan, C.R.; Ebersole, J.A. Two New Plioplatecarpine Mosasaurs (Mosasauridae: Plioplatecarpinae) of the Genus *Ectenosaurus* from the Upper Cretaceous of North America. *PaleoBios* **2023**, *40*, 1–28. [\[CrossRef\]](#)
57. Bell, G.L.; Barnes, K.R.; Polcyn, M.J. Late Cretaceous Mosasauroids (Reptilia, Squamata) of the Big Bend Region in Texas, USA. *Earth Environ. Sci. Trans. R. Soc. Edinb.* **2012**, *103*, 571–581. [\[CrossRef\]](#)
58. Bell, G.L.; Polcyn, M.J. *Dallasaurus turneri*, a New Primitive Mosasauroid from the Middle Turonian of Texas and Comments on the Phylogeny of Mosasauridae (Squamata). *Neth. J. Geosci.* **2005**, *84*, 177–194. [\[CrossRef\]](#)
59. Lively, J.R. Taxonomy and Historical Inertia: *Clidastes* (Squamata: Mosasauridae) as a Case Study of Problematic Paleobiological Taxonomy. *Alcheringa Australas. J. Palaeontol.* **2018**, *42*, 516–527. [\[CrossRef\]](#)
60. Everhart, M.J. Revisions to the Biostratigraphy of the Mosasauridae (Squamata) in the Smoky Hill Chalk Member of the Niobrara Chalk (Late Cretaceous) of Kansas. *Trans. Kans. Acad. Sci.* **2001**, *104*, 59–78. [\[CrossRef\]](#)
61. Holwerda, F.M.; Mitchell, M.T.; Van De Kerk, M.; Schulp, A.S. Mosasaur Feeding Ecology from the Campanian Bearpaw Formation, Alberta, Canada: A Preliminary Multi-Proxy Approach. *Diversity* **2025**, *17*, 205. [\[CrossRef\]](#)
62. Russell, D.A. *A New Species of Globidens from South Dakota, and a Review of Globidentine Mosasaurs*; Fieldiana, Geology; Field Museum of Natural History: Chicago, IL, USA, 1975; Volume 33.
63. Schulp, A.S.; Polcyn, M.J.; Mateus, O.; Jacobs, L.L.; Morais, M.L. A New Species of *Prognathodon* (Squamata, Mosasauridae) from the Maastrichtian of Angola, and the Affinities of the Mosasaur Genus *Liodon*. In *Proceedings of the Second Mosasaur Meeting*; Fort Hays State University Fort Hays: Hays, KS, USA, 2008; Volume 3, pp. 1–12.
64. DeBraga, M.; Carroll, R.L. The Origin of Mosasaurs as a Model of Macroevolutionary Patterns and Processes. In *Evolutionary Biology*; Hecht, M.K., MacIntyre, R.J., Clegg, M.T., Eds.; Springer US: Boston, MA, USA, 1993; pp. 245–322, ISBN 978-1-4613-6248-7.

65. Polcyn, M.J.; Lindgren, J.; Bardet, N.; Cornelissen, D.; Verding, L.; Schulp, A.S. Description of New Specimens of *Halisaurus arambourgi* Bardet and Pereda Suberbiola, 2005 and the Relationships of Halisaurinae. *Bull. De La Société Géologique De Fr.* **2012**, *183*, 123–136. [\[CrossRef\]](#)
66. Polcyn, M.J.; Augusta, B.G.; Zaher, H. Reassessing the Morphological Foundations of the Pythonomorph Hypothesis. In *The Origin and Early Evolutionary History of Snakes*; Gower, D.J., Zaher, H., Eds.; Systematics Association; Cambridge University Press: Cambridge, UK, 2022; Volume Special Volume Series, pp. 125–156, ISBN 978-1-108-93889-1.
67. Koch, P.L.; Tuross, N.; Fogel, M.L. The Effects of Sample Treatment and Diagenesis on the Isotopic Integrity of Carbonate in Biogenic Hydroxylapatite. *J. Archaeol. Sci.* **1997**, *24*, 417–429. [\[CrossRef\]](#)
68. Passey, B.H.; Cerling, T.E.; Levin, N.E. Temperature Dependence of Oxygen Isotope Acid Fractionation for Modern and Fossil Tooth Enamels. *Rapid Comm Mass Spectrom.* **2007**, *21*, 2853–2859. [\[CrossRef\]](#)
69. Kusaka, S.; Nakano, T. Carbon and Oxygen Isotope Ratios and Their Temperature Dependence in Carbonate and Tooth Enamel Using a GasBench II Preparation Device: Letter to the Editor. *Rapid Commun. Mass Spectrom.* **2014**, *28*, 563–567. [\[CrossRef\]](#)
70. Swart, P.K.; Burns, S.J.; Leder, J.J. Fractionation of the Stable Isotopes of Oxygen and Carbon in Carbon Dioxide during the Reaction of Calcite with Phosphoric Acid as a Function of Temperature and Technique. *Chem. Geol. Isot. Geosci. Sect.* **1991**, *86*, 89–96. [\[CrossRef\]](#)
71. Chesson, L.A.; Kenyhercz, M.W.; Regan, L.A.; Berg, G.E. Addressing Data Comparability in the Creation of Combined Data Sets of Bioapatite Carbon and Oxygen Isotopic Compositions. *Archaeometry* **2019**, *61*, 1193–1206. [\[CrossRef\]](#)
72. Christiansen, P.; Bonde, N. A New Species of Gigantic Mosasaur from the Late Cretaceous of Israel. *J. Vertebr. Paleontol.* **2002**, *22*, 629–644. [\[CrossRef\]](#)
73. Polcyn, M.J.; Jacobs, L.L.; Schulp, A.S.; Mateus, O. The North African Mosasaur *Globidens phosphaticus* from the Maastrichtian of Angola. *Hist. Biol.* **2010**, *22*, 175–185. [\[CrossRef\]](#)
74. Mateus, O.; Polcyn, M.J.; Jacobs, L.L.; Araújo, R.; Schulp, A.S.; Marinheiro, J.; Pereira, B.; Vineyard, D. Cretaceous Amniotes from Angola: Dinosaurs, Pterosaurs, Mosasaurs, Plesiosaurs, and Turtles. In Proceedings of the V International Conference on Dinosaur Paleontology and their Environment, Salas de los Infantes, Burgos, 26 July 2012; pp. 71–105.
75. Lindgren, J. Dental and Vertebral Morphology of the Enigmatic Mosasaur *Dollosaurus* (Reptilia, Mosasauridae) from the Lower Campanian (Upper Cretaceous) of Southern Sweden. *Bull. Geol. Soc. Den.* **2005**, *52*, 17–25. [\[CrossRef\]](#)
76. Fernandez, M.; Martin, J.E. Description and Phylogenetic Relationships of *Taniwhasaurus antarcticus* (Mosasauridae, Tylosaurinae) from the Upper Campanian (Cretaceous) of Antarctica. *Cretac. Res.* **2009**, *30*, 717–726. [\[CrossRef\]](#)
77. Fischer, V.; Bennion, R.F.; Foffa, D.; MacLaren, J.A.; McCurry, M.R.; Melstrom, K.M.; Bardet, N. Ecological Signal in the Size and Shape of Marine Amniote Teeth. *Proc. R. Soc. B Biol. Sci.* **2022**, *289*, 20221214. [\[CrossRef\]](#) [\[PubMed\]](#)
78. Jagt, J.W.; Mulder, E.W.; Dortangs, R.W.; Kuypers, M.; Peeters, H.; Verding, L. Recent Additions to the Late Maastrichtian Mosasaur Faunas of Liège-Limburg (The Netherlands, Belgium). *Sargetia (Acta Musei Devensis Ser. Sci. Naturae)* **2002**, *19*, 13–26.
79. Dortangs, R.W.; Schulp, A.S.; Mulder, E.W.A.; Jagt, J.W.M.; Peeters, H.H.G.; De Graaf, D.T. A Large New Mosasaur from the Upper Cretaceous of The Netherlands. *Neth. J. Geosci.* **2002**, *81*, 1–8. [\[CrossRef\]](#)
80. Clementz, M.T. *Sea Cows, Seagrasses, and Stable Isotopes: Biogeochemical Evaluation of the Ecology and Evolution of the Sirenia and Desmostylia*; University of California: Santa Cruz, CA, USA, 2002.
81. Clementz, M.T.; Fox-Dobbs, K.; Wheatley, P.V.; Koch, P.L.; Doak, D.F. Revisiting Old Bones: Coupled Carbon Isotope Analysis of Bioapatite and Collagen as an Ecological and Palaeoecological Tool. *Geol. J.* **2009**, *44*, 605–620. [\[CrossRef\]](#)
82. Lee-Thorp, J.A.; Sealy, J.C.; Van Der Merwe, N.J. Stable Carbon Isotope Ratio Differences between Bone Collagen and Bone Apatite, and Their Relationship to Diet. *J. Archaeol. Sci.* **1989**, *16*, 585–599. [\[CrossRef\]](#)
83. Tieszen, L.L.; Fagre, T. Effect of Diet Quality and Composition on the Isotopic Composition of Respiratory CO₂, Bone Collagen, Bioapatite, and Soft Tissues. In *Prehistoric Human Bone*; Lambert, J.B., Grupe, G., Eds.; Springer: Berlin/Heidelberg, Germany, 1993; pp. 121–155, ISBN 978-3-662-02896-4.
84. Toperoff, A.K. *Examination of Diet of Harbor Porpoise (Phocoena phocoena) from Central California Using Stomach Content and Stable Isotope Analysis from Multiple Tissues*; San Jose State University: San Jose, CA, USA, 2002.
85. Walker, J.L.; Macko, S.A. Dietary Studies of Marine Mammals Using Stable Carbon and Nitrogen Isotopic Ratios of Teeth. *Mar. Mammal Sci.* **1999**, *15*, 314–334. [\[CrossRef\]](#)
86. Mendes, S.; Newton, J.; Reid, R.J.; Frantzis, A.; Pierce, G.J. Stable Isotope Profiles in Sperm Whale Teeth: Variations between Areas and Sexes. *J. Mar. Biol. Assoc. UK* **2007**, *87*, 621–627. [\[CrossRef\]](#)
87. Rey-Iglesia, A.; Wilson, T.; Routledge, J.; Skovrind, M.; Garde, E.; Heide-Jørgensen, M.P.; Szpak, P.; Lorenzen, E.D. Combining $\delta^{13}\text{C}$ and $\delta^{15}\text{N}$ from Bone and Dentine in Marine Mammal Palaeoecological Research: Insights from Toothed Whales. *Isot. Environ. Health Stud.* **2023**, *59*, 66–77. [\[CrossRef\]](#)
88. Benner, R.; Biddanda, B.; Black, B.; McCarthy, M. Abundance, Size Distribution, and Stable Carbon and Nitrogen Isotopic Compositions of Marine Organic Matter Isolated by Tangential-Flow Ultrafiltration. *Mar. Chem.* **1997**, *57*, 243–263. [\[CrossRef\]](#)

89. Boeuf, B.J.L.; Crocker, D.E.; Grayson, J.; Gedamke, J.; Webb, P.M.; Blackwell, S.B.; Costa, D.P. Respiration and Heart Rate at the Surface Between Dives in Northern Elephant Seals. *J. Exp. Biol.* **2000**, *203*, 3265–3274. [\[CrossRef\]](#)
90. Truchot, J.-P. *Comparative Aspects of Extracellular Acid-Base Balance*; Zoophysiology; Springer: Berlin/Heidelberg, Germany, 1987; Volume 20, ISBN 978-3-642-83132-4.
91. Randall, D.J.; Burggren, W.W.; French, K.; Eckert, R. *Eckert Animal Physiology: Mechanisms and Adaptations*, 5th ed.; W.H. Freeman and Co: New York, NY, USA, 2002; ISBN 978-0-7167-3863-3.
92. Lutz, P.L.; Storey, K.B. Adaptations to Variations in Oxygen Tension by Vertebrates and Invertebrates. In *Comprehensive Physiology*; Prakash, Y.S., Ed.; Wiley: Hoboken, NJ, USA, 1997; pp. 1479–1522, ISBN 978-0-470-65071-4.
93. Ackerman, R.; White, F. Cyclic Carbon Dioxide Exchange in the Turtle *Pseudemys scripta*. *Physiol. Zool.* **1979**, *52*, 378–389. [\[CrossRef\]](#)
94. Lutcavage, M.E.; Lutz, P.L. Diving Physiology. In *The Biology of Sea Turtles*; Lutz, P.L., Musick, J.A., Eds.; CRC Press: Boca Raton, FL, USA, 1997; Volume 1, p. 410, ISBN 978-0-203-73708-8.
95. McConnaughey, T.A.; Burdett, J.; Whelan, J.F.; Paull, C.K. Carbon Isotopes in Biological Carbonates: Respiration and Photosynthesis. *Geochim. Et Cosmochim. Acta* **1997**, *61*, 611–622. [\[CrossRef\]](#)
96. Biasatti, D.M. Stable Carbon Isotopic Profiles of Sea Turtle Humeri: Implications for Ecology and Physiology. *Palaeogeogr. Palaeoclimatol. Palaeoecol.* **2004**, *206*, 203–216. [\[CrossRef\]](#)
97. Roe, L.J.; Thewissen, J.G.M.; Quade, J.; O’Neil, J.R.; Bajpai, S.; Sahni, A.; Hussain, S.T. Isotopic Approaches to Understanding the Terrestrial-to-Marine Transition of the Earliest Cetaceans. In *The Emergence of Whales*; Thewissen, J.G.M., Ed.; Springer: Boston, MA, USA, 1998; pp. 399–422, ISBN 978-1-4899-0161-3.
98. Lindgren, J. Stratigraphical Distribution of Campanian and Maastrichtian Mosasaurs in Sweden—Evidence of an Intercontinental Marine Extinction Event? *GFF* **2004**, *126*, 221–229. [\[CrossRef\]](#)
99. Lindgren, J.; Siverson, M. The First Record of the Mosasaur *Clidastes* from Europe and Its Palaeogeographical Implications. *Acta Palaeontologica Polonica* **2004**, *49*, 219.
100. Jagt, J.W.M. Stratigraphic Ranges of Mosasaurs in Belgium and the Netherlands (Late Cretaceous) and Cephalopod-Based Correlations with North America. *Neth. J. Geosci.* **2005**, *84*, 283–301. [\[CrossRef\]](#)
101. Mulder, E.W.A.; Formanoy, P.; Gallagher, W.B.; Jagt, J.W.M.; Schulp, A.S. The first North American record of *Carinodens belgicus* (Squamata, Mosasauridae) and correlation with the youngest in situ examples from the Maastrichtian type area: Palaeoecological implications. *Neth. J. Geosci.* **2013**, *92*, 145–152. [\[CrossRef\]](#)
102. Wendler, I. A Critical Evaluation of Carbon Isotope Stratigraphy and Biostratigraphic Implications for Late Cretaceous Global Correlation. *Earth Sci. Rev.* **2013**, *126*, 116–146. [\[CrossRef\]](#)
103. Cavin, L.; Tong, H.; Boudad, L.; Meister, C.; Piuze, A.; Tabouelle, J.; Aarab, M.; Amiot, R.; Buffetaut, E.; Dyke, G.; et al. Vertebrate Assemblages from the Early Late Cretaceous of Southeastern Morocco: An Overview. *J. Afr. Earth Sci.* **2010**, *57*, 391–412. [\[CrossRef\]](#)
104. Grigoriev, D. Redescription of *Prognathodon lutugini* (Squamata, Mosasauridae). *Proc. Zool. Inst. RAS* **2013**, *317*, 246–261. [\[CrossRef\]](#)
105. Gilmore, C.W. A New Mosasauroid Reptile from the Cretaceous of Alabama. *Proc. United States Natl. Mus.* **1912**, *41*, 479–484. [\[CrossRef\]](#)
106. Martin, J.E. A New Species of the Durophagous Mosasaur *Globidens* (Squamata: Mosasauridae) from the Late Cretaceous Pierre Shale Group of Central South Dakota, USA. In *The Geology and Paleontology of the Late Cretaceous Marine Deposits of the Dakotas*; Special Paper; Geological Society of America: Boulder, CO, USA, 2007; pp. 177–198, ISBN 978-0-8137-2427-0.
107. Dollo, L. Nouvelle Note Sur Les Vertébrés Fossiles Récemment Offerts Au Musée de Bruxelles Par M. Alfred Lemonnier. *Bull. Société Belg. Géologie Paléontologie Et D’hydrologie* **1889**, *3*, 214–215.
108. Schulp, A.S.; Polcyn, M.J.; Mateus, O.; Jacobs, L.L. Two Rare Mosasaurs from the Maastrichtian of Angola and the Netherlands. *Neth. J. Geosci.* **2013**, *92*, 3–10. [\[CrossRef\]](#)
109. Woodward, A.S. III.—Note on Tooth of an Extinct Alligator (*Bottosaurus belgicus*, sp. nov.) from the Lower Danian of Ciply, Belgium. *Geol. Mag.* **1891**, *8*, 114–115. [\[CrossRef\]](#)
110. Thurmond, J. New Name for the Mosasaur *Compressidens* Dollo, 1924. *J. Paleontol.* **1969**, *43*, 1298.
111. Bardet, N.; Suberbiola, X.P.; Iarochène, M.; Amalik, M.; Bouya, B. Durophagous Mosasauridae (Squamata) from the Upper Cretaceous Phosphates of Morocco, with Description of a New Species of *Globidens*. *Neth. J. Geosci.* **2005**, *84*, 167–175. [\[CrossRef\]](#)
112. Lingham-Soliar, T. Mosasaurs from the Upper Cretaceous of Niger. *Palaeontology* **1991**, *34*, 653–670.

Disclaimer/Publisher’s Note: The statements, opinions and data contained in all publications are solely those of the individual author(s) and contributor(s) and not of MDPI and/or the editor(s). MDPI and/or the editor(s) disclaim responsibility for any injury to people or property resulting from any ideas, methods, instructions or products referred to in the content.